M.Sc. Thesis
Meteorology

WATER VAPOR CORRECTION FUNCTIONS FOR CO_2 AND CH_4 IN CAVITY RING-DOWN SPECTROSCOPY

Mika Korkiakoski

February 24, 2014

Supervisor: Juha Hatakka (FMI)

Reviewers: Juha Hatakka (FMI) and Timo Vesala

UNIVERSITY OF HELSINKI
DEPARTMENT OF PHYSICS

P.O. BOX 64 (Gustaf Hällströmin katu 2)
FIN-00014 University of Helsinki

HELSINGIN YLIOPISTO – HELSINGFORS UNIVERSITET – UNIVERSITY OF HELSINKI

Tiedekunta/Osasto – Fakultet/Sektion – Faculty	Laitos – Institution – Department
Faculty of Science	Department of Physics

Tekijä – Författare – Author
Mika Korkiakoski

Työn nimi – Arbetets titel – Title

Water vapor correction functions for CO_2 and CH_4 in cavity ring-down spectroscopy

Oppiaine – Läroämne – Subject
Meteorology

Työn laji – Arbetets art – Level	Aika – Datum – Month and year	Sivumäärä – Sidoantal – Number of pages
M.Sc. Thesis	February 2014	45 pp. + appendices 5 pp.

Tiivistelmä – Referat – Abstract

Cavity ring-down spectroscopy is a laser absorption technique based on the principle of measuring the rate of exponential decay of light intensity inside the ring-down cavity. When the absorption spectrum of a gas is known, it is possible to determine the mole fraction of this gas by measuring the height of the absorption peak, which can be acquired from the rate of decay of light. This technique is used in G1301, G2301 and G2401 (Picarro Inc.) gas analyzers which measure carbon dioxide (CO_2), methane (CH_4) and water vapor. However, measured gas mole fractions are diluted from their actual value; mostly due to variations in atmospheric water vapor. This effect causes large errors and it has to be corrected either by drying the sample or applying a water vapor correction. A default water vapor correction is included in Picarro gas analyzers, but it might not be accurate enough for use in some measurements.

In this study, determination of water vapor correction coefficients was carried out by doing several droplet tests for seven different gas analyzers, which included one G2401, two G1301, four G2301gas analyzers. Mean correction functions determined for the analyzers were compared to the Picarro default correction. In addition, the comparison was made with time series data for one of the analyzers. Also, the water vapor measurement of the gas analyzers was calibrated to acquire the actual water vapor mole fraction.

As a result, the factory correction for CO_2 was proved sufficient for high accuracy measurements only up to 0.7 % water vapor mole fraction. For CH_4, the factory coefficient was enough up to 2.0 %, which corresponds to dew point temperature of 18 °C. In conclusion, neither of factory corrections is enough for use all year round. So, the water vapor correction should be made for each gas analyzer when making high accuracy measurements. Due to cyclic drift of water vapor measurement, the correction should remain stable over time, but this needs further verification. Currently, the correction should be made at least once per year.

Avainsanat – Nyckelord – Keywords
cavity ring-down spectroscopy, water vapor correction, water vapor calibration, carbon dioxide, methane, greenhouse gas

Säilytyspaikka – Förvaringställe – Where deposited
Kumpula Campus library, University of Helsinki

Muita tietoja – Övriga uppgifter – Additional information

HELSINGIN YLIOPISTO – HELSINGFORS UNIVERSITET – UNIVERSITY OF HELSINKI

Tiedekunta/Osasto – Fakultet/Sektion – Faculty	Laitos – Institution – Department
Matemaattis-luonnontieteellinen tiedekunta	Fysiikan laitos

Tekijä – Författare – Author
Mika Korkiakoski

Työn nimi – Arbetets titel – Title

Water vapor correction functions for CO_2 and CH_4 in cavity ring-down spectroscopy

Oppiaine – Läroämne – Subject
Meteorologia

Työn laji – Arbetets art – Level	Aika – Datum – Month and year	Sivumäärä – Sidoantal – Number of pages
Pro gradu -tutkielma	Helmikuu 2014	45 s. + liitteet 5 s.

Tiivistelmä – Referat – Abstract

Ontelovaimenemisspektroskopia on absorptiomenetelmä, jossa mitataan valon intensiteetin eksponentiaalista vaimenemista useita voimakkaasti heijastavia peilejä sisältävässä ontelossa. Kun tiedetään kaasun absorptiospektri, niin pystytään määrittämään kaasun mooliosuus mittaamalla absorptiopiikin korkeutta, mikä saadaan valon intensiteetin vaimenemisnopeudesta. Tätä tekniikkaa käytetään G1301, G2301 and G2401 -kaasuanalysaattoreissa (Picarro Inc.), jotka mittaavat hiilidioksidin, metaanin ja vesihöyryn mooliosuuksia. Mittausten ongelmana on kaasujen mooliosuuksien laimeneminen, joka johtuu pääosin ilmakehän vesihöyryn määrän vaihtelusta. Tämä ilmiö aiheuttaa suuria virheitä ja se täytyy korjata joko kuivaamalla näyte ennen mittausta tai tekemällä vesihöyrykorjaus. Korjaus on sisäänrakennettu Picarron valmistamissa kaasuanalysaattoreissa, mutta tämä tehdaskorjaus ei välttämättä ole riittävä mittauksissa, joissa tarvitaan suurta tarkkuutta.

Tässä tutkielmassa vesihöyrykorjaus suoritettiin kahdelle G1301, neljälle G2301 ja yhdelle G2401 -kaasuanalysaattorille tekemällä jokaiselle muutama pisarakoe. Pisarakokeista saaduista korjausfunktioista laskettiin keskiarvot eri analysaattoreille, mitä verrattiin tehdaskorjauksen arvoihin. Lisäksi vertailu tehtiin yhden kaasuanalysaattorin kohdalla myös aikasarja-analyysin avulla. Kaikille kaasuanalysaattoreille tehtiin myös vesihöyrykalibrointi, jotta saatiin selville todellinen vesihöyryn mooliosuus.

Hiilidioksidin tehdaskorjaus osoittautui riittäväksi, mikäli vesihöyryn mooliosuus on alle 0.7 %. Metaanille tehdaskorjaus oli riittävä 2.0 % mooliosuuteen asti, mikä vastaa 18 °C kastepistelämpötilaa. Kumpikaan näistä tehdaskorjauksista ei ole riittävä ympärivuotiseen mittaamiseen, joten on suositeltavaa tehdä vesihöyrykorjaus erikseen jokaiselle kaasuanalysaattorille, jotta mittauksen tarkkuus olisi mahdollisimman hyvä. Vesihöyrymittauksen ryömintä on laitetekniikasta johtuen jaksottainen, joten vesihöyrykorjauksen pitäisi pysyä stabiilina ajan kanssa, mutta tätä ei ole vielä vahvistettu. Tällä hetkellä vesihöyrykorjaus tulisi tehdä vähintään kerran vuodessa.

Avainsanat – Nyckelord – Keywords
ontelovaimenemisspektroskopia, vesihöyrykorjaus, vesihöyrykalibrointi, hiilidioksidi, metaani, kasvihuonekaasu

Säilytyspaikka – Förvaringställe – Where deposited
Kumpulan tiedekirjasto, Helsingin yliopisto

Muita tietoja – Övriga uppgifter – Additional information

Contents

1 Introduction

Climate change is one of the biggest challenges humankind is facing today and in near future. Climate change is mainly caused by increased mole fractions (Appendix A) of greenhouse gases; mainly of carbon dioxide (CO_2) and methane (CH_4) (Kiehl et al., 1997; Forster et al., 2007; Montzka et al., 2011). The researchers working with the climate change need measurements of very high precision and accuracy to produce results which, for example, can be used to make better climate models (Huntingford et al., 2009), understand global carbon cycle (Tans et al., 1996) and quantify the contributions of CH_4 sources and sinks (Crutzen, 1991) which currently have high uncertainty (Houweling et al., 2006; Frankenberg et al., 2008). However, the problem with traditional greenhouse gas measurements has been that they had to be carried out for dry gas samples, which meant building an expensive and possibly complex drying system (Rella, 2010). The drying has to be made to counter the dilution and spectral line broadening effects which cause significant change in mole fractions of CO_2 and CH_4 with changing the amount of water vapor in the air (e.g. Rella et al., 2012).

In recent years, a new set of greenhouse gas analyzers using cavity ring-down spectroscopy (CRDS) has been commercialized. Unlike the traditional gas analyzers using, for example, non-dispersive infrared (NDIR) sensor, CRDS analyzers are able to carry out more stable and precise measurements of CO_2 and CH_4 even without drying the gas (Crosson, 2008; Chen et al., 2010; Richardson et al., 2011; Stephens et al., 2011). The simultaneous water vapor measurement allows for the post correction of CO_2 and CH_4 mole fractions made for moist gas (e.g. Rella, 2010; Rella et al., 2012). This makes it possible to achieve the inter-laboratory compatibility values set by Global Atmospheric Watch (GAW) program of the World Meteorological Organization (WMO) for CO_2 and CH_4 (WMO, 2011). In northern hemisphere, the compatibility limits are ±0.1 ppm for CO_2 and ±2 ppb for CH_4. In southern hemisphere, the limits are half of the values in northern hemisphere. Traditionally, reaching these limits has required very dry gas streams with dew point temperatures below -39°C (WMO, 2011; Rella et al., 2012).

The objective of this study is to determine the water vapor correction coefficients for CO_2 and CH_4 and inspect, if they are transferrable between Picarro (Picarro Inc., USA) gas analyzers using wavelength-scanned cavity ring-down spectroscopy (WS-CRDS). The main goal is to test if using the factory functions is enough or is the instrument specific water vapor correction required. In addition, the water vapor mole fraction measured by the instrument is calibrated by calibration functions similar to those of the greenhouse gases. The water vapor correction coefficients are determined by investigating how much the instrument specific mole fractions of CO_2 and CH_4 decrease when the amount of water vapor in the air is increased. The coefficients are calculated for seven different gas analyzers and the transferability between these instruments is inspected by comparing Picarro factory functions, included in all Picarro gas analyzers, to the ones determined in this study. Picarro factory functions were applicable, if using them instead of instrument specific correction functions would keep the accuracy within the WMO limits.

Chapter 2 includes a short introduction to the laser absorption technique used by the gas analyzers in this study. Also, phenomena causing errors in greenhouse measurements are explained and how they can be corrected by deriving empirical water vapor correction functions. In Chapter 3, experiments and instruments used are described, in addition to data processing methods. Chapter 4 includes the results from the water vapor calibration and water vapor correction for the greenhouse gases and transferability of these functions is inspected as well. At the end of the chapter, problems encountered in the experiments are discussed and theories for reasons behind them are explained. Finally, Chapter 5 summarizes the results and discusses the ways to make the experiments more reliable.

2 Theory and background

In this chapter, first the Cavity ring-down spectroscopy technique is presented by explaining, how the absorption spectrum is obtained. Also, determination of sensitivity and description what happens inside an instrument during the measurement are included. The second part of this chapter consists of the reasons behind the need for water vapor correction and the derivation of the empirical water vapor correction functions.

2.1 Cavity ring-down spectroscopy

Cavity ring-down spectroscopy is a laser absorption technique developed by O'Keefe and Deacon (1988). This technique is based on the principle of measuring the rate of exponential decay of light intensity inside a stable optical resonator called the ring-down cavity (K. Busch and M. Busch, 1997). When the light with characteristic wavelength is put into the ring-down cavity from a laser source, the light is absorbed by the molecules of measured gas. Rest of the light is transmitted out of the cavity. The mole fraction or isotopic ratio of the sample can be found from the obtained absorption spectrum by calculating the difference between decay rates of an cavity without a sample and a cavity containing a sample, however, the line-shape parameters and the absorption cross-section of the gas must be known (e.g. Wheeler et al., 1998).

2.1.1 Obtaining absorption spectrum

In spectroscopic analysis, the most important processes are absorption and emission of electromagnetic radiation caused by atoms and molecules. Beer-Lambert law describes the absorption of light and connects together the intensity of a spectral feature and the frequency-dependent absorption properties of a gas sample (Bernath, 1995). Beer-Lambert law can be written as follows:

$$I = I_0 e^{-\sigma CL} \tag{1}$$

Where I_0 is the intensity of light entering the sample, I is the intensity of light leaving the sample, C is the mole fraction of the absorber, L is the path length of the sample and σ is the absorption cross-section of the sample at some wavelength. The product of C and σ can be expressed as the absorption coefficient α. In addition, the exponent is also defined as absorbance.

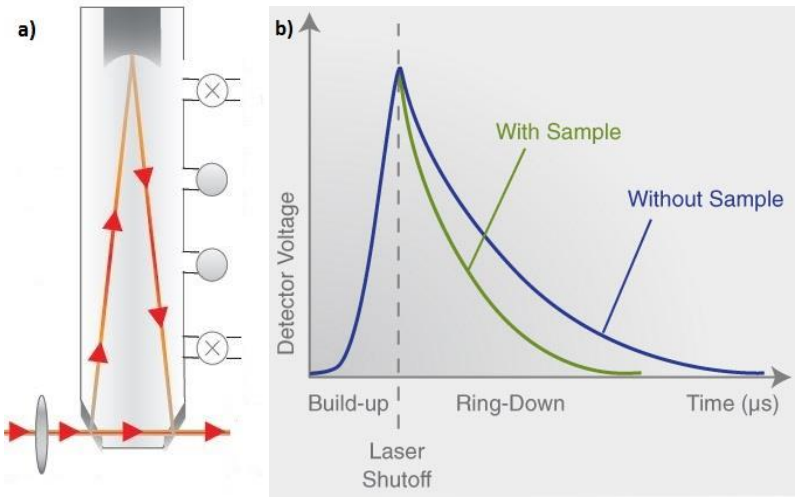

Figure 2.1. (a) Ring-down cavity and light travelling inside of it. Small amounts of light is transmitted through the mirrors on each reflection which can be measured by a detector. (Vaughn et al., 2008) (b) Transmitted light measured by a detector coming from an empty cavity (blue) and a cavity with a sample. (http://www.picarro.com/technology/cavity_ring_down_spectroscopy)

When the laser pulse is transmitted into the ring-down cavity, fraction of light leaves the cavity through the mirrors on each reflection (Figure 2.1a). When there is no absorber present, the intensity of light transmitted through the exit mirror decreases as a function of time according to the following equation (Wheeler et al., 1998):

$$I = I_0 e^{-\frac{t}{\tau_0}} \tag{2}$$

Where I_0 is the initial light intensity, t is time, τ_0 is the empty cavity ring-down time, which describes how long it takes for the intensity of light to reach $\frac{1}{e}$ of I_0 when only the reflectivity of the mirrors cause the decay of light (Figure 2.1b). Typical values are few

tens of microseconds for CRDS-instruments (Wheeler et al., 1998; Crosson, 2008). From now on, the decay of light is considered only on one wavelength and cavity modes are ignored as their effect is small (Berden and Engeln, 2009). During the trace gas measurement, the decay is proportional to the total optical losses inside the ring-down cavity including the round-trip scattering, mirror-transmission losses and the absorbance of a sample.

The empty cavity ring-down time can be approximated like follows (Wheeler et al., 1998):

$$\tau_0 = \frac{l}{c}|\ln(R)| \approx \frac{l}{c(1-R)} \tag{3}$$

Where c is the speed of light in vacuum, l is the distance between two mirrors and R is the mirror reflectivity. Losses inside cavity, for example, by mirror transmission, diffraction and scattering, are equal to $(1-R)$. These losses determine the empty cavity ring-down time which depends strongly on the reflectivity of the mirrors (e.g. Wheeler et al., 1998). In practice, the empty cavity ring-down time is not determined by removing the gas from the cavity, but by tuning the laser wavelength where the gas does not absorb the light (Picarro, 2010). If sample gas is included inside the cavity, and the wavelength of the light inside the cavity is the same as the absorption wavelength of the gas, the decay of light intensity increases and Equation 2 receives one additional term (Wheeler et al., 1998):

$$I = I_0 e^{-\frac{t}{\tau_0} - \alpha c t} \tag{4}$$

In which α is the molecular absorption coefficient $\left(\frac{1}{\{length\}}\right)$ and c is the speed of light. The product of c and t is the path length (L). With an absorber present, the new decay time (τ) is:

$$\tau = \tau_0 + \frac{1}{c\alpha} \tag{5}$$

To acquire the absorption spectrum, the decay curve is calculated for each laser wavelength. Usually, decay times are determined by making an exponential fit to a discrete decay curve and getting τ from it. When the empty cavity ring-down time is known, values of α for each laser wavelength can be determined. Finally, the absorption spectrum is obtained by plotting α against wavelength. However, this method requires that the decay is a true exponential, otherwise the values of α would be inaccurate. In addition, knowledge of the partial pressure of the absorbing species inside the cavity is required to acquire information about absorption cross-sections (Wheeler et al., 1998).

Measuring a decay rate and not absolute signal intensity is the reason why instruments using CRDS-technique have low calibration drift that is high accuracy and also high precision (Picarro, 2010). This means that neither short nor long-term drifts in laser power or detector response cause any effect between decay rate and sample gas mole fraction. In addition to measuring a decay rate, calibration drift can be minimized by keeping pressure and temperature inside the cavity constant and stable, so that gas does not respond to changes in ambient conditions. Also, if wavelength of the laser beam is modified to scan over the absorption spectrum, it is possible to monitor simultaneously multiple trace species and also increase measurement accuracy. Wavelength-scanning is a method which also increases measurement accuracy and eliminates the need for a reference gas (Silver, 1992). The combination of wavelength-scanning and CRDS-technique is called Wavelength-scanned cavity ring-down spectroscopy (WS-CRDS). The gas analyzers used in this study are WS-CRDS instruments.

2.1.2 Sensitivity

The non-invasive detection of trace species is the primary application of CRDS. When dealing with species existing in parts per million (ppm) or parts per billion (ppb) levels, it is crucial to have very high sensitivity to measure these low mole fractions precisely. The sensitivity of CRDS-technique is usually described as the smallest detectable change in absorption in ring-down time which is limited by the accuracy of the decay time measurement. According to Scherer et al. (1997), the theoretical limit of

uncertainty of decay time measurement is well below 1%, in practice, maximum of 1% uncertainty is easily achieved.

The quantity used to specify the sensitivity of CRDS is called the fractional loss of intensity per round trip (δI) (Wheeler et al., 1998). The absorption coefficient for a single pass through a cavity can be derived from Beer-Lambert law (Equation 1) by knowing that the absorption coefficient α is a product of σ and C. If we presume that the absorbances in one pass are very small ($\alpha l \ll 1$), we can conclude (Wheeler et al., 1998):

$$\delta I = \frac{I_0 - I}{I_0} \approx \alpha l \tag{6}$$

According to Zalicki and Zare (1995) the absorbance of one pass through cavity can be written as:

$$\alpha l = (1 - R)\frac{\tau_0 - \tau}{\tau} \tag{7}$$

When combining Equations 6 and 7, the minimum detectable fractional absorbance per pass can be written as follows:

$$\delta I_{min} = (1 - R)\frac{\Delta\tau_{min}}{\tau} = (1 - R)\frac{\Delta N_{min}}{N} \tag{8}$$

Where $\Delta\tau_{min}$ is the smallest detectable change in of absorption in ring-down time, in other words, the precision of $\Delta\tau$. N is the number of round trips in the cavity and ΔN_{min} is the accuracy of this quantity.

One way to increase the sensitivity is to increase the mirror reflectivity. As a result, increased reflectivity increases the path length and causes longer background decay time, therefore, making it possible to detect smaller relative changes in τ. On the other hand, this method requires higher powered lasers, so that smaller amount of light can be detected. CRDS measurements are independent of the initial light intensity. As a result,

shot to shot fluctuations of the laser pulses do not decrease sensitivity unlike with conventional absorption techniques (Wheeler et al., 1998). Sensitivity is typically reported as the minimum detectable fractional absorption per round trip of a laser because the number of round trips, therefore also the path length, depends on the strength of the absorbing species (Scherer et al., 1997). In other words, when absorption is strong, the ring-down time decreases which in turn reduces sensitivity. Other factors affecting the sensitivity are the noise of the laser and detector and the resolution of the detector.

2.1.3 Measuring mole fractions of CO_2 and CH_4

Almost all the small gas molecules have a unique near-infrared absorption spectrum (Picarro, 2010). The spectrums consist of a series of well-spaced, narrow sharp lines each on their own characteristic wavelengths. When the wavelengths of these lines are known, it is possible to determine the mole fraction of the species by measuring the height of the absorption peak on their specific wavelengths, in other words, the strength of absorption. The CRDS-technique enables the pathlength of many kilometers which makes it possible to measure the mole fractions on ppb level and some gases even on parts per trillion (ppt) levels.

The following components and measuring principles are explained based on Picarro (Picarro Inc, USA) gas analyzers. The three principal components making up a CRDS-instrument are: a laser, a photodetector and an optical cavity consisting of at least two mirrors (Crosson, 2008). Additionally, the system includes laser control electronics, wavelength monitor and data collection and electronics to analyze a sample (Figure 2.2). In greenhouse gas measurements, the analyzer uses two telecom-grade distributed feedback (DFB) lasers. The incoming light from the lasers is selected by using an optical switch and the light is moved to a wavelength monitor through a polarization maintaining optical fiber (Crosson, 2008). The first laser is used to measure CO_2 spectrum around a wavelength of 1603 nm and the second measures CH_4 and water vapor spectrum around 1651 nm wavelength. In newer analyzers (G2401), there is also a third laser which measures carbon monoxide (CO). The cavity is connected to a

sample pipeline and the flow rate of the sample (~250 ml/min) and pressure (186.65 hPa) inside the cavity is controlled by a critical orifice and an internal pressure controller. The photodetector measures the decay of the laser pulse inside the cavity in real-time.

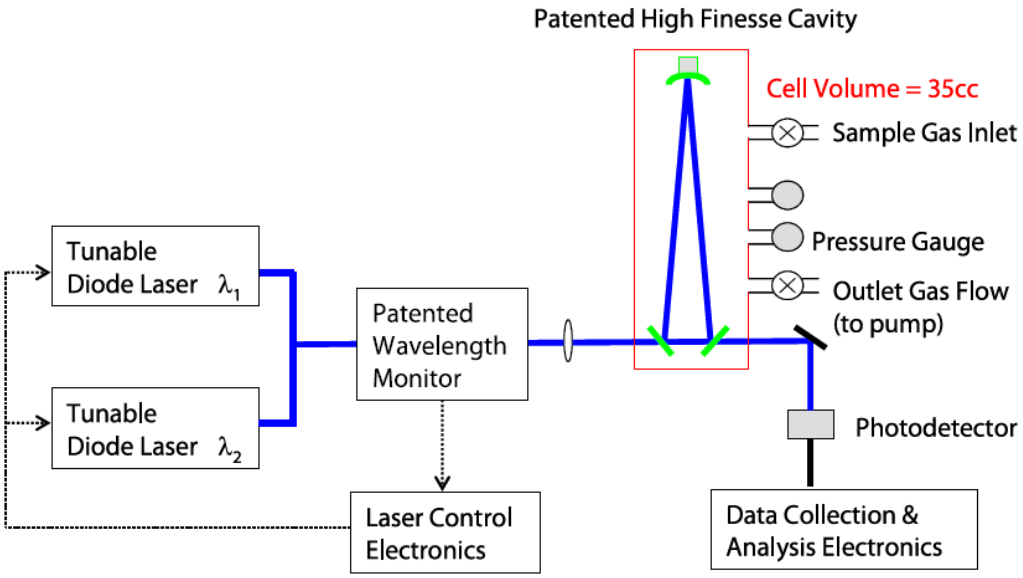

Figure 2.2. Basic components of a gas analyzer using CRDS-technique (Crosson 2008).

The mole fraction measurement starts by guiding light from the infrared laser source into the cavity through one of the partially reflecting mirrors (Crosson, 2008). The cavity is kept in constant pressure (~18.7 kPa) and temperature (318.15 K) with variations less than 13.3 Pa and 0.02 K, because the shapes of the spectral lines of CO_2 and CH_4 are sensitive to the fluctuations in temperature and pressure (Rella et al., 2012). In time, the light intensity increases; this is measured by the photodetector through the second, partially reflecting, mirror. When the intensity has built enough, the laser is turned off, which causes the intensity of the light to decrease exponentially (Figure 2.1b and Figure 2.3) while it is bouncing between the mirrors (e.g. Crosson, 2008; Picarro, 2010; Chen et al., 2010). During this phase, which is called the ring-down phase, the cavity ring-down time of the light intensity is measured (Chapter 2.1.1). Most of the light remains inside the cavity for few tens of microseconds producing long path lengths, even tens of kilometers (Picarro, 2010). With the cavity ring-down time, it is

possible to obtain the absorption spectra as described in Chapter 2.1.1, which is comprised of absorption loss versus optical frequency (Crosson, 2008). In the gas analyzers used in this study, the mole fraction is calculated from the absorption peak heights. The peak height method is used instead of the peak area to increase accuracy in measurements due to the systematic noise in the baseline and the noise in the wavelength measurement (Chen et al., 2010).

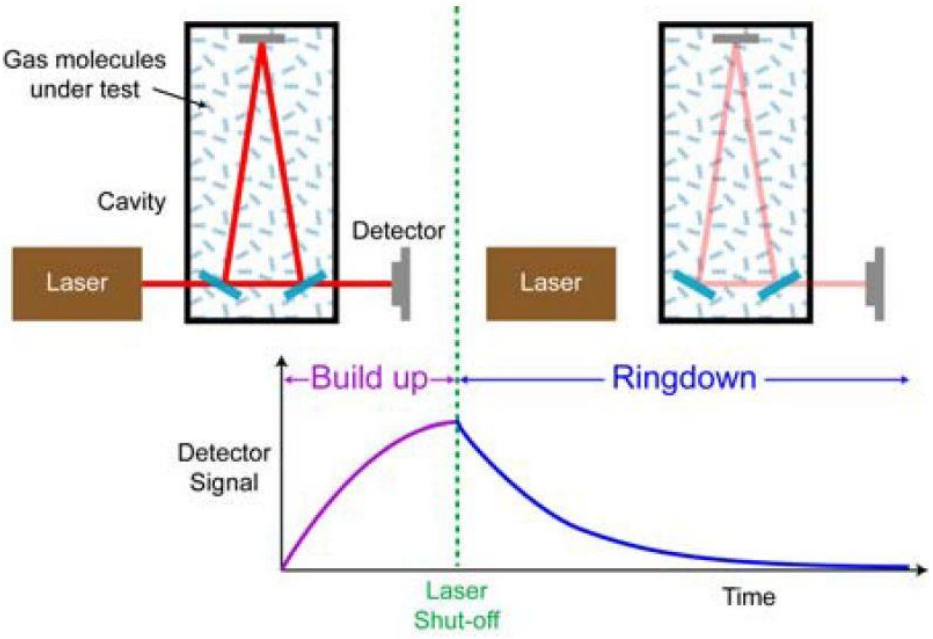

Figure 2.3. Schematic diagram of the cavity and the detector signal in laser build-up and in the ring-down phase where the laser is turned off. On upper left is the cavity with the sample gas and three mirrors in build-up phase. On upper right is the same thing, but in ring-down phase where the light is decaying and the decay rate is measured by the detector. On the bottom is the detector signal (light intensity) as a function of time. (Picarro, 2010)

2.2 Water vapor correction for CRDS-instruments

2.2.1 The dilution effect

The dilution effect is the largest error source in greenhouse gas measurements and it means a change in measured mole fractions of CO_2 and CH_4 mainly due to variations of atmospheric water vapor in the air. When the humidity is increased, the mole fractions of other gases will dilute meaning that their measured mole fraction decreases. The dilution effect happens, for example, when water evaporates from a liquid surface into the air, which increases amount of water vapor in air, consequently, diluting atmospheric gas mole fractions.

The variation in greenhouse gas mole fractions due to the dilution effect is not insignificant. The dilution effect is significant even on extremely low water vapor mole fractions. For example, achieving inter-laboratory compatibility values without the water vapor correction (Chapter 2.2.3) for CO_2 (±0.1 ppm) set by WMO (WMO, 2011), requires a water vapor mole fraction smaller than 0.021 %, which corresponds to -39 °C dew point temperature. There are not many places on the Earth where the dew point temperature ever decreases even as low as -30 °C, therefore, the dilution effect must always be corrected for the results.

To avoid consequences of the dilution effect, CO_2 and CH_4 mole fractions must be reported as dry mole fractions. These variations in water vapor mole fraction hide the atmospheric variation of greenhouse gases resulting from surface-atmosphere exchange fluxes (Rella et al., 2012). There are mainly two ways to acquire dry mole fractions of CO_2 and CH_4. First way is to dry the gas to very low dew point temperatures. There are many problems when drying gas sample, for example, it is expensive and it adds more complexity to the measurement system. The second method requires a gas analyzer which, in addition to greenhouse gas mole fractions, measures also water vapor mole fraction. When the dry mole fraction of CO_2 or CH_4 and the diluted mole fraction on different water vapor mole fractions is known, it is possible to derive an empirical correction function, which corrects the wet mole fractions to dry mole fractions.

2.2.2 Line broadening effects

The spectral line shape of isolated ro-vibrational lines used by CRDS-instruments is determined by three principal mechanisms: Doppler broadening, Lorentzian broadening and Dicke line narrowing (e.g. Varghese and Hanson, 1984; Rella, 2010). In addition, term pressure broadening is used for including Lorentzian broadening and Dicke line narrowing (Dicke, 1953) as they both are proportional to pressure. These mechanisms only affect the peak height; not the total area of the absorption line (Chen et al., 2010). In ambient air, only variations in water vapor mole fraction cause noticeable changes in these line broadening and narrowing parameters. Mole fractions of other gases, for example, oxygen, nitrogen and carbon dioxide, do not vary enough to produce any measurable changes (Chen et al., 2010). Also, water vapor mole fraction itself is affected by these line broadening effects, which causes nonlinearity of the reported water vapor mole fraction with respect to the true water vapor mole fraction (Rella, 2010).

Doppler broadening is caused by different velocities of molecules (e.g. Rautian and Sobel'man, 1967) in the gas sample. When the laser beam is moving inside the cavity, some of the molecules are moving in the same direction as the beam and some are moving to opposite direction. Due to these relative motions, a small frequency shift is produced. However, speed of the molecules depends on the temperature of the gas sample, therefore, line broadening is enhanced when temperature is increased. The line shape, which is Doppler broadened, approaches a Gaussian distribution which is related to the velocity of the molecule (Rella, 2010). However, the line shape approaches Gaussian distribution only if the pressure of the gas is low. Also, the width of the distribution depends on the velocity of the molecule. Doppler broadening does not depend on background gas composition and it is a property of the analyzed molecule.

Lorentzian broadening of the spectral line is caused by random collisions and thermal motion of the gas molecules surrounding the target molecule (Rella, 2010; Nara et al., 2012). These collisions disturb the structure of the molecule and broaden the spectral line, which is proportional to the pressure of the background gas matrix. Lorentzian

broadening can be parameterized by the Lorentzian line broadening parameter y (Varghese and Hanson, 1984; Rella, 2010). If both Doppler and Lorentzian broadening are taken into account, the line shape is said to follow a Voigt profile, which is a commonly used line profile (Rella, 2010). Unlike the Doppler broadening, the Lorentzian broadening depends on the background gas matrix, in addition to the analyzed molecules (Rella, 2010; Nara et al., 2012).

When dealing with high-precision spectroscopy, it is important to take line narrowing into account. Doppler line shape is enough on low pressures, but when the pressure is higher, the molecules collide more frequently and they break the Gaussian line shape (Rella, 2010). This causes the spectral line to narrow which strengthens the peaks, while weakening the other part of the spectrum. There are several ways to model this effect, for example, Galatry profile (Galatry, 1961) which is used in the Picarro WS-CRDS gas analyzers. The Galatry profile uses a single parameter called the Galatry line-narrowing parameter z which is proportional to the pressure a background gas (Varghese and Hanson, 1984; Rella, 2010). Line narrowing coefficient is a property of the analyzed molecules and it depends on the composition of the background gas, however, it is derived from fundamentally different processes as the Lorentzian broadening coefficient, which makes them independent of each other for different background gas compositions. The line narrowing correction is small compared to Lorentzian broadening and it has been found out that it is possible to set z to be proportional to y (Rella, 2010; Nara et al., 2012).

The effect of these line broadening and narrowing effects is not insignificant. If they are not corrected, they can cause a systematic error which can be even 40% of the dilution effects (Appendix B) when utilizing CO_2 and CH_4 lines used in CRDS-analyzer (Rella, 2010). However, the CRDS-technique measures CO_2, CH_4 and water vapor with high precision, so it is possible to derive empirical functions to describe the dry gas mole fractions of CO_2 and CH_4 with respect to measured water vapor mole fraction. All these line broadening and narrowing effects can be put into a single empirical expression, therefore, it is unnecessary to understand each effect separately.

2.2.3 Derivation of the empirical correction functions

To determine the empirical water vapor correction functions for CO_2 and CH_4, the measurement of water vapor mole fraction must be highly precise to maintain high precision in measured dry gas mole fractions. According to Rella (2010), if the CO_2 uncertainty is wanted to be kept less than 0.05 ppm on a 400 ppm level, the water vapor mole fraction measurement must be accurate to a level of 0.0125 % (125 ppm). The wet and dry gas mole fractions are related with water vapor mole fraction as follows (Rella, 2010; Rella et al., 2012):

$$\frac{C_{diluted}}{C_{dry}} = 1 - 0.01H_{act} \tag{9}$$

Where C is the diluted and the dry mole fractions of the species (CO_2 or CH_4) and H_{act} is the actual water vapor mole fraction (%). The term -0.01 comes from the expected dilution effect. To avoid the use of this equation, as it requires very precise measurements of H_{act} and $C_{diluted}$, it is better to determine the empirical functions which relate the diluted mole fractions of CO_2 and CH_4 and the water vapor mole fraction reported by the instrument to the dry mole fractions of CO_2 and CH_4. It is possible to determine the dry gas mole fractions without calibrating the water vapor measurement by using correct experimental methods.

Rella et al. (2012) found out how the water vapor affects the peak heights of the analyzed molecule and how it is proportional to the peak height of the analyzed gas. In addition, they noticed that this effect can be modeled by doing a Taylor series expansion to water vapor mole fraction. By keeping the terms up to the second order, the line shape effect can be described by the following equation:

$$\frac{C_{wet}}{C_{diluted}} = 1 + x_1 H_{act} + x_2 H_{act}^2 \tag{10}$$

Where C_{wet} is the mole fraction of the species in humid gas and x and x_2 are the first and second order correction coefficients.

Water vapor spectral line is affected by a phenomenon called self-broadening. It is similar to the line broadening effects affecting CO_2 and CH_4 spectrum as it is also happening due to changes in water vapor mole fraction and causes nonlinearity in the measurements. H_{act} and water vapor mole fraction measured by instrument (H_{rep}) can be related by the following expression, which is derived from the peak height of the water vapor spectral line, while keeping all terms up to second order after Taylor series expansion (Rella et al., 2012):

$$H_{act} = y_1 H_{rep} + y_2 H_{rep}^2 \tag{11}$$

Where y_1 and y_2 are the first and second order correction coefficients for the water vapor. One method to determine these coefficients is described in Chapter 3.2.

As a result, combining Equations 9, 10 and 11 gives:

$$\frac{C_{wet}}{C_{dry}} = 1 + z_1 H_{rep} + z_2 H_{rep}^2 \tag{12}$$

C_{wet}, C_{dry} and H_{rep} can be measured by proper experiments. One possible experiment is explained in Chapter 3.3. When C_{wet}, C_{dry} and H_{rep} are measured, it is possible to determine z_1 and z_2 empirically without knowing the constants in Equations 10 and 11 first. This means that it is not required to know how the line shape changes the spectral line of the target gas. In addition, water vapor measurements do not need to be highly accurate anymore, only high precision and stability is required (Rella et al., 2012). In other words, as long as H_{rep} is well-behaved and increases as a function of the actual water vapor mole fraction (H_{act}), it is suitable equivalent for measuring actual water vapor when correcting CO_2 and CH_4 measurements.

3 Methods

In this chapter, the Picarro gas analyzers using WS-CRDS-technique are introduced briefly; concentrating in differences between the instruments as the more technical description of CRDS-technique was given in Chapter 2.1. Also, the experimental procedures used to determine the correction coefficients for CO_2, CH_4 and water vapor (H_2O) are explained. And finally, the data post-processing methods made for droplet tests and water vapor calibrations are explained shortly.

3.1 Picarro gas analyzers

The water vapor correction coefficients for CO_2 and CH_4 were determined for seven different gas analyzers (Table 3.1). In addition, the water vapor calibration was carried out for all these instruments. The gas analyzers were based on WS-CRDS technology (Chapter 2.1) manufactured by Picarro (Picarro Inc., USA). The group of gas analyzers consisted of three different series: G1301 (and one G1301-m), G2301 and G2401. G1301 was released in 2006 and was the first commercial instrument of this type made by Picarro. One of these older instruments (G1301-m) used in the experiments was a model for airborne measurements with increased durability to vibrations and added ambient pressure sensor and correction for wavelength monitor (Chen et al., 2010). Common notation for these modified instruments is an extra "-m" after the series name (Table 3.1). G2301 is a second generation instrument which has been available since 2010. It uses the same core optical spectrometer as the G1301 with almost identical performance characteristics (Rella et al., 2012), but the package and the pump system is new. Finally, the newest series G2401 has all the same features as the two previous series, but it also measures CO. However, carbon monoxide has been disregarded in following measurements as the dilution and spectral effects are internally corrected for CO in Picarro analyzers.

Table 3.1. The instruments and their model number used in this study.

Instrument	CFADS100	CFDDS101	CFADS2130	CFADS2135	CFADS2237	CFADS2242	CFKADS2066
Model	G1301	G1301-m	G2301	G2301	G2301	G2301	G2401

3.2 Water vapor calibration

Water vapor calibration should always be made for instruments measuring water vapor mole fraction due to, for example, self-broadening effects of the water vapor spectral line shape. However, water vapor calibration is not required for dilution and spectral effect corrections for CO_2 or CH_4, so it can be made if accurate water vapor results are wanted. The method described below to acquire the calibration coefficients takes around an hour depending on the interval and the range of dew point temperatures used.

The measurement system is visualized in Figure 3.1. To produce a humidified gas stream, dry compressed ambient air (Technical air, AGA Oy, FIN) from a cylinder was guided through an absolute pressure regulator (Type 640, MKS Instruments, USA) into the dew-point generator (LI-610, LiCor, USA). The dew-point generator was used to generate a gas stream with different water vapor mole fractions by changing the dew point temperature. The total flow rate was adjusted so that the overflow was ~250 ml/min. The flow rate of Picarro analyzer was ~250 ml/min. The overflow was measured by a flow meter (Veri-flow 500, Agilent Technologies, USA).

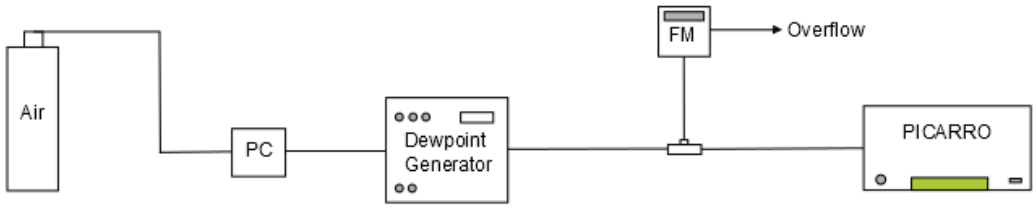

Figure 3.1. The test setup for determining water vapor calibration functions. PC is the pressure controller and FM is the flow meter.

At the start of the experiment, the dew-point generator was set to humidify the gas stream with 0.15 °C dew point temperature. Reaching this value took some time but after that, increasing the dew point temperature and waiting for the generator to set to the new temperature took less than a minute. The dew point range used was 0.15–23.00 °C and the measured dew points were: 0.15°C, 5.00°C, 10.00°C, 15.00°C, 19.00°C and 23.00°C. On every dew point, water vapor mole fraction was measured for ten minutes

before switching to next dew point temperature.

Also, two separate tests were carried out to check accuracy of the dew point temperature shown by the generator. This was made by using a chilled mirror hygrometer (Dewmaster, EDGE Tech, USA) to measure the dew point temperature generated by the generator. Chilled mirror hygrometers work well as a calibration standard as they are most stable instruments in long term for humidity measurements (Heinonen, 2006). The hygrometer was set in parallel with the gas analyzer while the rest of the setup was kept the same (Figure 3.1). The flow between the gas analyzer and the hygrometer was divided equally so that the flow for each of the instruments was ~250 ml/min. It was noticed that the generator could not generate low 0–5 °C nor high >22 °C dew point temperatures accurately which therefore had to be corrected. This is explained in Chapter 3.4.1.

3.3 Water droplet test

The method to determine the water vapor correction coefficients for CO_2 and CH_4 is called “water droplet test”. The droplet test consists of humidifying a dry gas stream by adding a droplet of ultra-pure water in the sample line. Ultra-pure water should always be used to avoid the effects of dissolved CO_2. Humidifying the gas stream causes the dilution and line broadening effects (Chapter 2.2), which can be corrected by measuring the dry mole fraction of the measured gas and the wet mole fractions at different water vapor mole fractions.

The method used to carry the water droplet tests is depicted in Figure 3.2. Dried gas used in this experiment was the same as in water vapor calibration –compressed ambient air from a cylinder. Synthetic air was not used because it has been proven to be not suitable for determining correction coefficients (Chen et al., 2010). A dry gas stream from the cylinder with constant mole fractions of CO_2 and CH_4 was guided through an absolute pressure controller (Type 640, MKS Instruments, USA) and from there to the Tee-system. This Tee-system consisted of 1/2" T-connector (Swagelok, USA), heating cable with temperature sensor and a power supply (Type 9320, Mascot, NOR). In

addition, one part of the Tee was sealed by a Nut (Swagelok, USA) except when the droplets were introduced. The power supply was used to heat the Tee-connector to reach higher water vapor mole fractions. A multimeter (179, Fluke, USA) with the temperature sensor, was used to measure the temperature of the Tee-connector. After few experiments, the multimeter was not used anymore due to the fact that measuring the temperature was not very useful which will be explained in results section.

The pressure difference between inside and outside of the pipeline was measured by a pressure gauge (CPG1000, WIKA Instrument, USA) before the dry gas stream reaches the Tee-connector. The pressure was adjusted with the pressure controller so that the pressure was slightly lower in the pipeline than the ambient (~ -110±10 hPa). Keeping the pressure difference negative provided a possibility to test for leaks in the measurement system. If there was a leak, it could be found more easily because the room air leaks to the pipeline and contaminates the gas stream, thus increasing the CO_2 mole fraction.

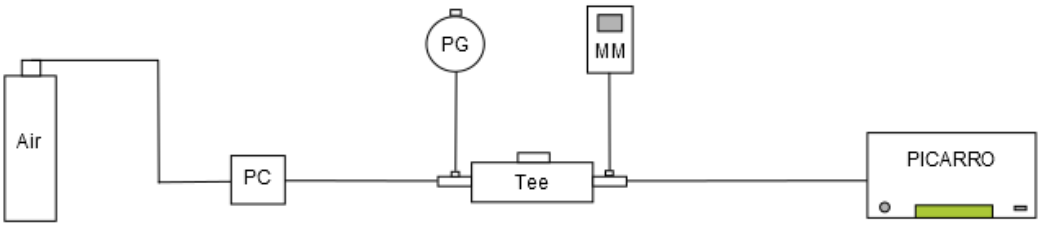

Figure 3.2. The test setup for determining water vapor correction functions for CO_2 and CH_4. PC is the pressure controller, PG is the pressure gauge and MM is the multimeter.

The gas analyzer had to be started some time before the experiment so it had enough time to warm up and stabilize. This took usually from 30 minutes up to 90 minutes. After the analyzer warmed up, it was connected to the measurement system and the gas cylinder was opened to measure the dry gas stream for at least 15 minutes. This gave the dry mole fractions of CO_2 and CH_4 which are needed for determining the correction coefficients (Equation 12).

The experiment began by disconnecting the nut from the Tee-connector and ten

droplets, which correspond to about 240 µl, of ultra-pure water (Milli-Q, Millipore Corporation) were injected into the Tee-connector with a syringe. The humidity of the gas stream depends on the temperature of the Tee-connector, and the water vapor mole fraction usually rose up to 1.4–1.5 % in room temperature (23–24 °C). The aim was to reach as high water vapor mole fraction as possible without causing condensation inside the pipeline, which happens when dew point temperature is the same as the room temperature. So, the target water vapor mole fraction was selected to be 2.5 %, which corresponds to ~21 °C dew point temperature. This gave some room for error. Tee-connector had to be heated to reach this water vapor mole fraction. The connector was heated until the water vapor mole fraction reached ~2.0 % and after that the heater was turned off. The temperature of the Tee-connector at 2.0 % was usually ~35 °C and max temperature reached shortly after that was ~37 °C. As a result, water vapor mole fraction reached usually ~2.5–3.0 % before starting to decrease. Usually, it took 2.5 hours for the system to dry up completely. After the system had dried up, the dry mole fractions of CO_2 and CH_4 were measured again for 15 minutes.

3.4 Transferability from a time series data

One way to test transferability of the water vapor correction coefficients is by using time series data. In this study, a time series data of CO_2, CH_4 and reported water vapor mole fraction were used. The measurements were made on the roof of Finnish Meteorological Institute (FMI) headquarters (60.20°N, 24.96°E, 54 m above sea level) for the period from 1 July 2011 to 30 June 2013 by CFADS100. The measurement site is about 4 km from Helsinki centrum in an urban area in the vicinity of sea where anthropogenic effects impact much on the measured greenhouse gas mole fractions.

The time series data was averaged over one minute and the most noticeable spikes were removed. Then the data of CO_2 and CH_4 were corrected by the mean of correction coefficients (Table C.1) determined from three droplet tests carried out for CFADS100. Also, the data was corrected with factory coefficients and the differences in mole fraction between the instrument specific and the factory correction were compared.

3.5 Data processing

3.5.1 Water vapor calibration

Only data required for determining the water vapor calibration coefficients, are the actual water vapor mole fraction of the gas stream and the water vapor mole fraction reported by the gas analyzer. However, it was checked whether that the dew point temperatures shown by the generator were correct and it was calibrated against a hygrometer (Table 4.1). This calibration was used for the dew point generator.

To acquire the calibration coefficients, the dew point temperatures were transformed to water vapor mole fractions by using the equation proposed by Goff (1957). It is based on Goff-Gratch equation (Goff and Gratch, 1946) and is recommended by WMO (WMO, 2012) to calculate saturation vapor pressures. The equation is written as follows:

$$\begin{aligned} log_{10(e_{w,s})} = {} & 10.79574\left(1-\frac{T_1}{T}\right) - 5.02800 log_{10}\left(\frac{T}{T_1}\right) \\ & + 1.50475 * 10^{-4}\left[1 - 10^{-8.2969\left(\frac{T}{T_1}-1\right)}\right] \\ & + 0.42873 * 10^{-3}\left[10^{4.76955\left(1-\frac{T_1}{T}\right)} - 1\right] \\ & + 0.78614 \end{aligned} \tag{13}$$

where T_1 = 273.16 K, $e_{w,s}$ is in hectopascals. Equation has been confirmed in the range 0–100°C, but the error should not be significant over super-cooled water in the range -50–0°C (WMO, 2012). Using definition of logarithm and dividing Equation 13 by 10, saturation water vapor pressure is received in %:

$$e_{w,s} = \frac{10^{log_{10}(e_{w,s})}}{10} \tag{14}$$

Next, the water vapor mole fractions calculated from the dew point temperatures were

plotted against the water vapor mole fraction reported by the gas analyzer. Finally, a quadratic fit was made to these six (Chapter 3.3) measurement points by using the least squares method, and the fit was forced to go through origin. The constants of this quadratic equation are the calibration coefficients. In addition, R^2 value was calculated to check the quality of the fit. Forcing through origin was justified by the fact that the analyzers reported 0±0.003 % water vapor mole fraction when measuring dry gas. The possible error in true water vapor mole fraction caused by forcing through origin is then less than 0.001 %.

3.5.2 Water droplet test

Before analyzing the data, one minute averages were calculated from the raw data and this averaged data was used to calculate the water vapor correction coefficients. To determine the correction coefficients, the ratio of mole fractions in the wet and dry gas streams $\frac{C_{wet}}{C_{dry}}$ was calculated for the water vapor range about 0.0–3.0 % depending on how high the water vapor mole fraction rose. C_{wet} is the CO_2 or CH_4 mole fraction reported by the instrument during the droplet evaporation. C_{dry} is the CO_2 or CH_4 average mole fraction reported by the instrument in dry gas stream before and after a droplet test. These mole fraction ratios of CO_2 and CH_4 were plotted against the water vapor mole fraction reported by the instrument. However, first three minutes following the introduction of the droplet were usually discarded for the calculations, because the water vapor mole fraction changed too fast. Quadratic equations were fitted to these datasets by using the least squares method. In addition, the fits were forced through the point when $H_{rep} = 0$ and $\frac{C_{wet}}{C_{dry}} = 1$. The coefficients of these quadratic equations are the water vapor correction coefficients (Equation 12). In addition, the quality of the fits was estimated by calculating R^2 values and plotting residual errors of the fits.

4 Results

In this chapter, the results of the measurements made in this study are shown and explained. First, the calibration coefficients for the water vapor mole fraction reported by the instrument are calculated to find the actual mole fraction. Second, the water vapor correction coefficients for CO_2 and CH_4 are calculated for the Picarro gas analyzers. Next, the calculated correction coefficients are compared with each other and against the factory coefficients used in the analyzers. The main goal is to test if one can use the factory coefficients and still have enough accuracy to meet the WMO requirements, or are the instrument specific coefficients required. Finally, there is a brief overview of the problems encountered in the measurements.

4.1 Water vapor calibration coefficients

The water vapor mole fraction reported by the instrument is not the actual water vapor mole fraction and it has to be calibrated to acquire the actual water vapor mole fraction. However, the actual water vapor mole fraction is not required for water vapor correction of CO_2 or CH_4 and it should be made only if one is interested in the actual water vapor results.

The water vapor calibration measurement, described in Chapter 3.2, was carried out once for every instrument, and it was also made twice against a hygrometer to check the accuracy of the dew point generator. The dew point temperatures measured by the dew point generator and the hygrometer are shown in Table 4.1. In these measurements, it was assumed that the hygrometer was “the golden standard”; the instrument showing the correct dew point temperature. Table 4.1 shows that the dew point generator could not generate accurately low and high dew point temperatures. The difference is high on the lowest dew point temperatures and it would cause high errors in results, if the temperature shown by the dew point generator was used. The rest of the measurements were carried out without the hygrometer, but the results were corrected with the dew point temperatures shown by the hygrometer in the first two measurements. This was justified by generating the same dew point temperatures in every measurement and by

the fact that the dew point temperatures shown by the hygrometer were same in both measurements it was used.

Table 4.1. Dew point temperatures measured by the dew point generator and hygrometer.

Dew point temperature (°C)	
Dew point generator	Hygrometer
0.15	0.50
5.00	5.20
10.00	10.10
15.00	15.00
19.00	19.00
23.00	22.80

Table 4.2. The coefficients (y_1 is linear and y_2 is quadratic) for Equation 11 *acquired from water vapor calibration tests and R^2 value of the fit for each gas analyzer.*

Instrument	y_1	y_2	R^2
CFADS100	0.768	0.04893	0.9999
CFDDS101	0.815	0.01425	1.0000
CFKADS2066	0.795	0.02738	0.9997
CFADS2130	0.798	0.01803	1.0000
CFADS2135	0.959	0.02691	0.9999
CFADS2237	0.792	0.02697	0.9997
CFADS2242	0.810	0.02019	0.9999

A sample plot made for CFADS2242 is shown in Figure 4.1 (upper panel). The quadratic fit made to the data points is the calibration equation:

$$H_{act} = 0.02656H_{rep}^2 + 0.796H_{rep} \quad (14)$$

So the water vapor calibration coefficients for CFADS2242 are: y_1 = 0.796 and y_2 = 0.02656. R^2 was 0.99997 and the residuals are shown in Figure 4.1 (lower panel).

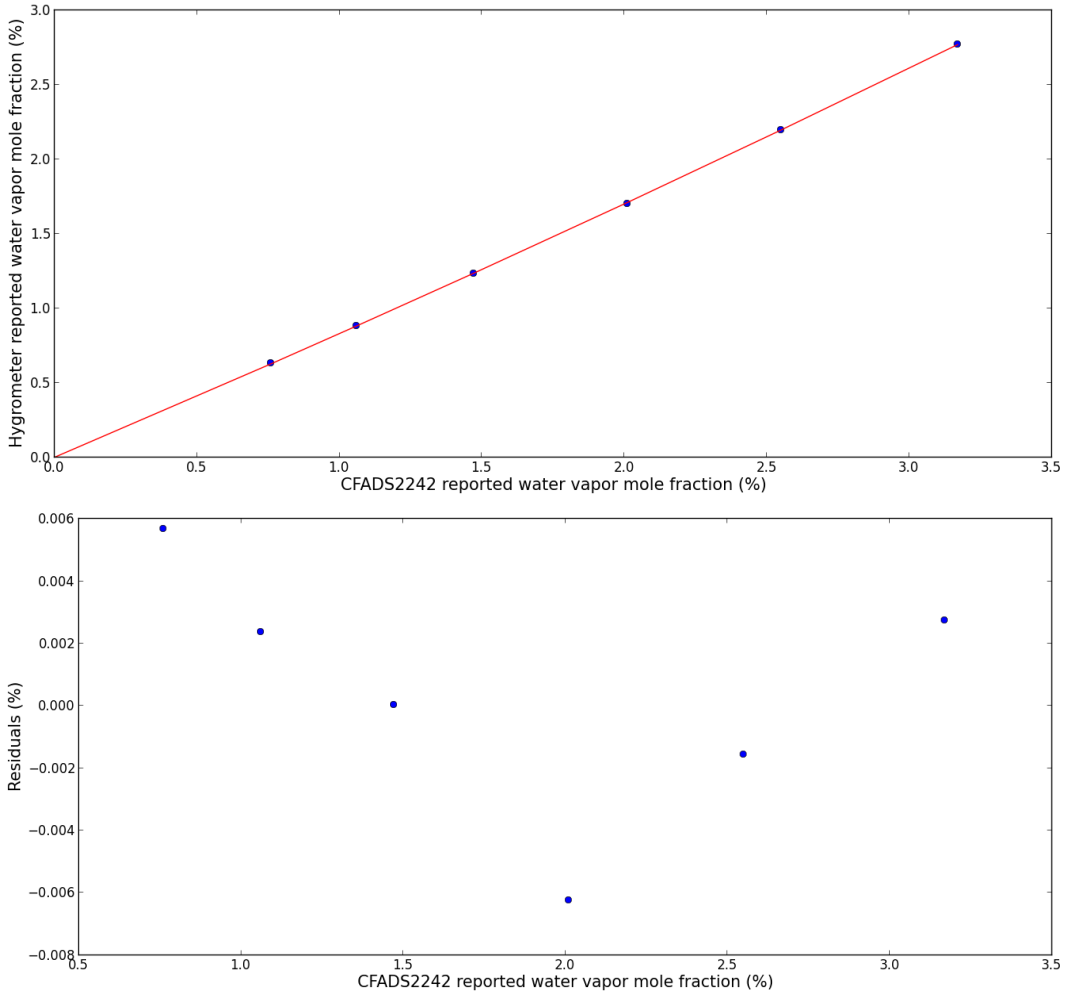

Figure 4.1. Water vapor mole fraction reported by the hygrometer plotted with respect to water vapor mole fraction measured by CFADS2242 and the residuals of the fit. R^2 value was 0.9997.

Rella (2010) defined the following calibration coefficients for water vapor: y_1 = 0.772 and y_2 = 0.01949. The coefficients determined for all gas analyzers are shown in Table 4.2. The linear coefficients (Table 4.2, second column) are in fairly good agreement with each other, but are slightly larger than the value presented by Rella (2010), which is probably due to a normal variation between the instruments. However, the difference of CFADS2135 compared to other analyzers is so large that there could be something wrong with the water vapor measurement in that instrument. The possible effect of these coefficients for water vapor correction coefficients is inspected in Chapter 4.3.

4.2 Water vapor correction coefficients for CO_2 and CH_4

CFADS2242 is used as an example instrument in this study to illustrate the results, but the resulting plots look similar also for the other analyzers. In upper panel of Figure 4.2, one minute averages of $\frac{CO_{2wet}}{CO_{2dry}}$ are plotted against the water vapor mole fraction reported by the gas analyzer. In this case, the ratio between wet and dry mole fractions decreased to around 0.970 for CO_2 and to 0.975 for CH_4 at 2.5 % water vapor mole fraction, corresponding to a dilution of gas mole fraction of 12 ppm for CO_2 and 45 ppb for CH_4. Quadratic fit made to the measurement points is colored red (Figure. 4.2) and the equation has a form:

$$\frac{CO_{2_{wet}}}{CO_{2_{dry}}} = -0.0002206H_{rep}^2 - 0.01214H_{rep} + 1 \quad (15)$$

According to Equation 12, the water vapor correction coefficients for CO_2 are: z_1= -0.01214 and z_2= -0.0002206. Quality of the fit was determined by calculating R^2 value, which in this case was 0.9999 and plotting the residuals (Figure 4.2, lower panel) which are all within ±0.04 ppm. Similar fit was made for CH_4 (Figure 4.3) and the quadratic equation was:

$$\frac{CH_{4_{wet}}}{CH_{4_{dry}}} = -0.0001902H_{rep}^2 - 0.01013H_{rep} + 1 \quad (16)$$

Thus, the coefficients for CH_4 were: z_1= -0.01013 and z_2 = -0.0001902. R^2 value was 0.9996 and the residuals were within ±0.7 ppb (Figure 4.3, lower panel). The water vapor correction coefficients of all instruments used in this study are categorized in Table C.1 (Appendix C).

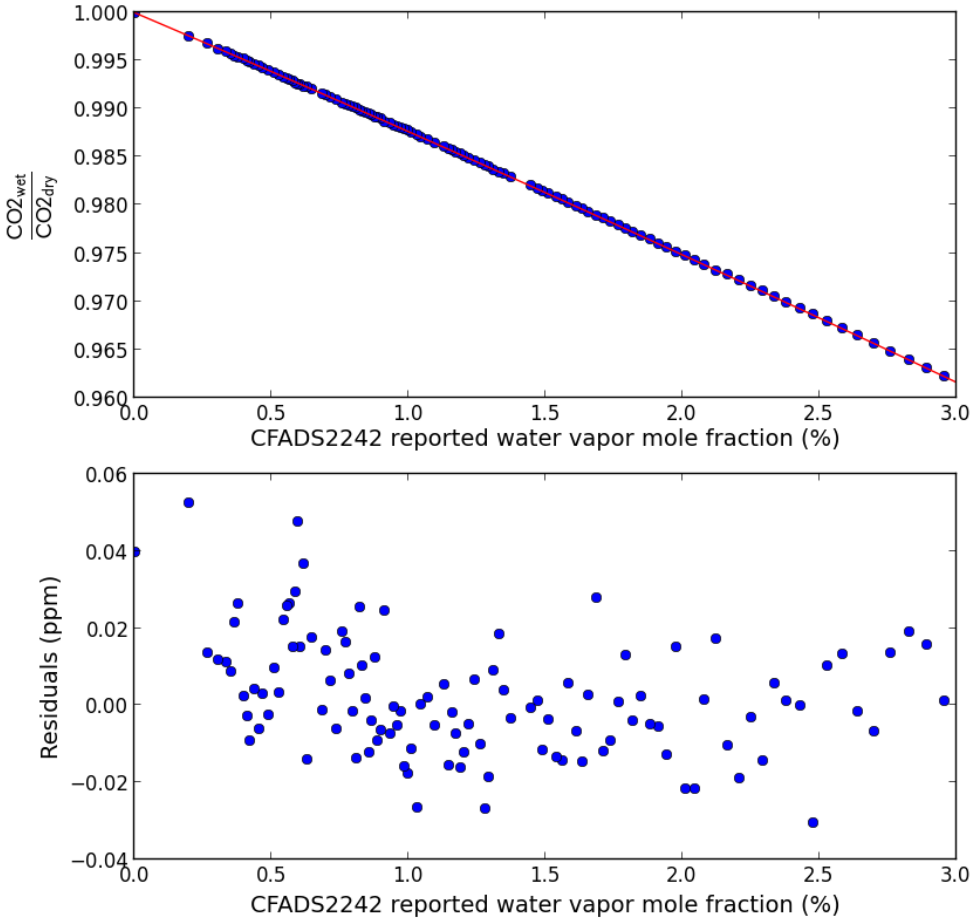

Figure 4.2. Quadratic fit of $\frac{CO_{2wet}}{CO_{2dry}}$ *versus reported water vapor mole fractions and residuals of the fit for CFADS2242.*

Mean values for water vapor correction coefficients were calculated for each of these gas analyzers by using the coefficients calculated from the water droplet tests which had higher R^2 value than 0.999. The water droplet test was made for seven different gas analyzers for 3–6 times (Table C.1) depending on the availability of the analyzer. If both CO_2 and CH_4 results had low R^2, they were excluded from Table C.1. Three out of four excluded tests were made for CFADS2237 and one for CFADS2130. In Table C.1, the coefficients marked with red color are excluded from the calculated mean due to bad fit. This meant that R^2 was < 0.999 and typically highest residuals were ±0.2 ppm for

CO_2 and ±1 ppb for CH_4. Possible reasons for these failed measurements are discussed in Chapter 4.4. Also, standard error of the mean was calculated for every mean coefficient, although, the statistical significance of these uncertainties with most of the analyzers is questionable because of low number of the droplet tests made.

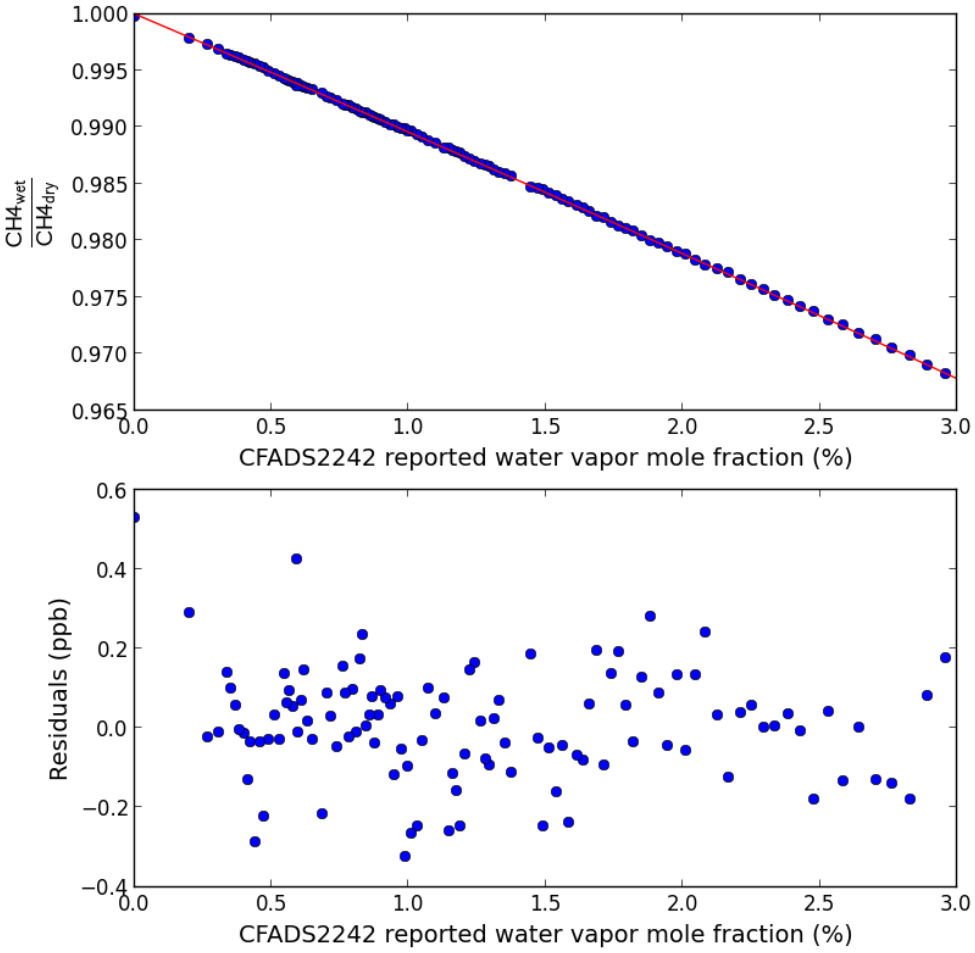

Figure 4.3 Quadratic fit of $\frac{CH_{4wet}}{CH_{4dry}}$ *versus reported water vapor mole fractions and residuals of the fit for CFADS2242.*

The second order coefficient can be approximated to be zero on low water vapor mole fractions, so it is possible to use a linear correction function to make the water vapor correction and still meet the WMO requirements. For CO_2, the second order coefficient starts to be meaningful somewhere between 0.7–0.8 % (2–4 °C dew point) depending on the magnitude of the coefficient. At these water vapor mole fractions, the CO_2 mole

fraction difference between using and not using second order coefficient becomes larger than 0.05 ppm. For CH_4, we can ignore the second order coefficient up to 1.8 % (16 °C dew point) when the difference between using and not using is <1 ppb for the highest second order term acquired from the experiments (CFADS100, Table C.1). On the other hand, for some of the instruments the second order coefficient of CH_4 was one order of magnitude smaller which makes the coefficient insignificant up to 3.6 % (27 °C dew point) water vapor mole fraction.

The uncertainties of the mean coefficients vary significantly between the instruments. The uncertainty of mole fraction corresponding to the uncertainties of the coefficients varies from 0.03 ppm (CFADS2135) to 0.13 ppm (CFADS2242) for CO_2 and from 0.34 ppb (CFDDS101) to 0.96 ppb (CFADS2242) for CH_4 at 2 % water vapor mole fraction. The uncertainty is large on some of the coefficients, therefore, more water droplet tests should have been made for them, especially for CFADS2237 and CFADS2242.

The stability of these corrections over time could be tested, but according to Rella (2010), the Picarro analyzers are guaranteed to be stable to 1 part in 800 over one month and it depends directly on the stability of the reported water vapor mole fraction. Also, the drift does not increase or decrease monotonically over time, but it rather cycles around the mean value due to the nature of technology (Rella, 2010). So, assuming a maximum error of 1 part in 400 on water vapor measurement, the largest error caused to CO_2 measurement at 400 ppm is 0.0125 ppm and 0.05 ppb for CH_4 at 2 ppb. If the instruments are calibrated and they are working properly, the water vapor correction should be stable over time to reach the WMO requirements.

4.3 Applicability of the Picarro factory correction functions

Due to the fact that all water droplet tests were carried out under the same experimental conditions and equipment, we can compare the water vapor correction coefficients determined for different instruments. As a result, it is possible to investigate if the correction functions are transferable between different instruments. This has been investigated by several research groups (Chen et al., 2010; Nara et al., 2012; Rella et al.,

2012) with different results. Chen et al (2010) showed that the correction function is transferable between WS-CRDS instruments when they corrected water vapor measurements of the G1301 to those of G1301-m. However, the statistics were weak because only two analyzers were tested. In contrast, Nara et al. (2012) could not verify the transferability of the correction functions, but they presumed that it was due to the experimental uncertainty. Rella et al. (2012) confirmed transferability up to 1.0 % water vapor mole fraction. With higher humidity levels, it was recommended to determine the correction coefficients independently for each instrument.

The factory (default) coefficients used in Picarro gas analyzers were determined by Chen et al. (2010) for water vapor range 0.6–6 % for a G1301 series instrument. These factory coefficients are: z_1 = -0.01200 ± 0.00009 and z_2 = -0.0002674 ± 0.000018. While investigating the applicability of the factory functions, we want to ensure that uncertainties and the error caused by using different correction functions stay under the inter-laboratory compatibility values set by WMO. It was decided that the limits should be half of the WMO limits in northern hemisphere to ensure transferability; 0.05 ppm for CO_2 and 1 ppb for CH_4, which are illustrated as red lines in Figure 4.4. As long as the plot of an instrument stays between those red lines, the error of using the Picarro factory coefficients is less than 0.05 ppm for CO_2 and less than 1 ppb for CH_4. In addition, when the uncertainties are taken into account the total accuracy should fulfill the requirements set by the WMO. It should also be noted, that when the lines of two gas analyzers stay within the limits it does not necessarily mean that the correction coefficients of the first analyzer are transferable with the second analyzer or vice versa.

The top panel in Figure 4.4 illustrates the difference of water vapor calibration functions compared to the function described by Rella (2010). The figure shows that most of the functions stay close to each other except CFADS2135 and CFADS100, which behave differently from others. The difference in CFADS100 coefficients might be due to the warmer measurement environment, but it is also possible that it is just normal variation between the instruments. However, the coefficients of CFADS2135 differ from others so much that there must be something different with the water vapor measurement of the analyzer. The measurements were made twice for the analyzer, but the results

remained same.

The middle panel in Figure 4.4 shows the difference in the mean water vapor correction function for CO_2 of different instruments to the factory function with respect to water vapor mole fraction reported by the analyzer when using $CO_{2_{dry}}$= 400 ppm. There are two instruments, CFADS100 and CFDDS101, which differ from the others right from the beginning. The interesting thing about this is that they both are series G1301 instruments as was the analyzer used by Chen et al. (2010). However, the fact that the only two G1301 series analyzers differ from other G2xx series is probably just due to normal variation between the instruments. The analyzers of series G2301 and one of G2401 seemed to differ much less from the factory coefficients. The curves of G2xxx series stay within the boundaries up to ~2.0 %. If the two G1301 series analyzers which differ much from other five analyzers were ignored, one can say that the factory functions are applicable up to 2.0 % water vapor mole fraction in air, which corresponds to ~18°C dew point temperature (Equation 13). This is not high enough for use, except maybe on some arctic and Antarctic stations (Vinther et al., 2006; Bromwich et al., 2012).

However, there is no good excuse to ignore these older analyzers, because the deviation of the correction coefficients derived from three droplet tests is small for both the instruments. Of course, results of three measurements are not enough for determining statistical significance, but in this case three stable results should be enough especially when the difference to the factory coefficients is so large. This ends up to conclusion that the factory coefficients are usable up to 0.7 % reported water vapor mole fraction, which corresponds to ~2°C dew point temperature.

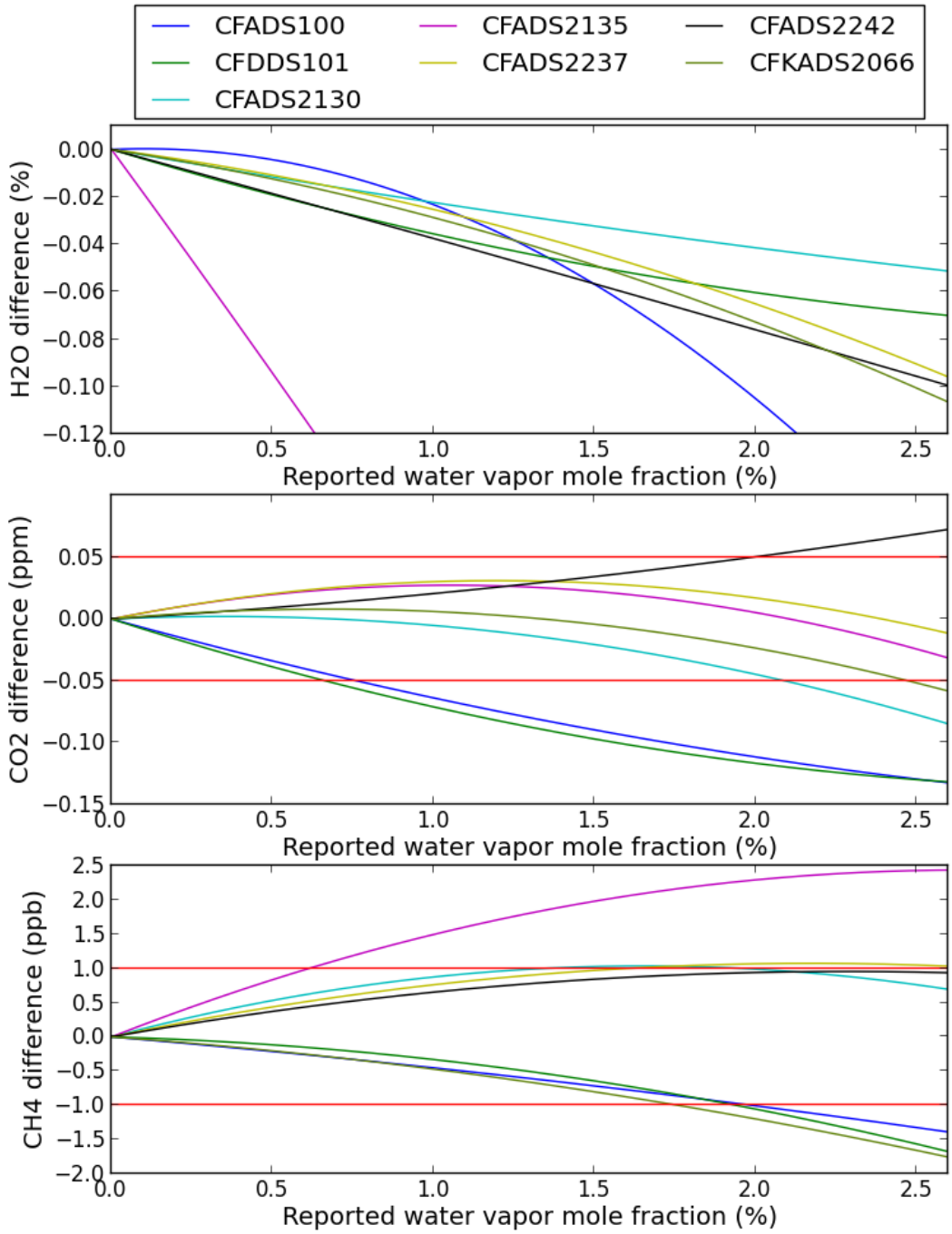

Figure 4.4. The first panel illustrates the difference in water vapor mole fraction between the water vapor calibration function (Table 4.2) defined for different analyzers to the function of Rella (2010). Next two panels show the difference of the mean water vapor functions (Table 4.1) for CO_2 and CH_4 to the Picarro factory coefficients. The outer red lines describe the precision limits (±0.05 ppm for CO_2 and ±0.001 ppm for CH_4). Horizontal axis for all panels is reported water vapor mole fraction of an analyzer.

The factory coefficients seem to differ somewhat with the results in Table 4.1. There are few minor differences, for example, some of the second order coefficients in Table C.1 are one order of magnitude smaller. In contrast, these analyzers have higher linear coefficient than the others with larger second order coefficient. Overall, most of the coefficients are not very close to the factory coefficients. This is illustrated in the bottom panel in Figure 4.4, which shows the same thing as the middle panel, but now for CH_4 using $CH_{4_{dry}}$ = 1.9 ppm. The analyzers are split to two "groups": the first group has both G1301 instruments, but unlike with CO_2, it now also includes CFKADS2066. The second group has the rest of the analyzers except CFADS2135 which seems to differ from others similarly as in water vapor calibration (Figure 4.4, top panel). So it might be possible that the water vapor measurement is causing some bias in CH_4 measurement. If CFADS2135 is ignored from the inspection, the factory coefficients would be usable up to 1.7 % reported water vapor mole fraction corresponding to dew point temperature of 15°C, which is significantly higher than with CO_2 coefficients.

CFADS2135 was used to carry out six water droplet tests in total which is the largest amount in this study. However, one of the CH_4 measurements was discarded due to bad fit, i.e. the residuals were too large. Comparing the water vapor coefficients to the factory coefficients reveals that the correction function for CO_2 stays well within the precision boundaries up to 2.6 % water vapor mole fraction (Figure 4.4, middle panel) and the coefficients seem to be the most stable ones compared to other instruments in this study (Table C.1). In contrast, CH_4 correction function (Figure 4.4, bottom panel) appears to be less accurate even though the coefficients are also quite stable like CO_2 coefficients. The linear coefficient of CH_4 is easily the largest of all the gas analyzers and the effect of that can be seen in Figure 4.4. One hypothesis is that the difference in water vapor measurements might affect to the water vapor correction coefficients. It could be possible to derive the correction coefficients from water vapor calibration coefficients, if strong enough relationship between them could be found. However, qualitative analysis shows that there seems to be no such relationship between them because the difference in water vapor mole fraction is always negative (Figure 4.4, first panel), but the difference in CO_2 (Figure 4.4, second panel) and CH_4 (Figure 4.4,

bottom panel) functions can be either negative or positive. In addition, if the reason was water vapor calibration, the CO_2 coefficients should have been affected as well.

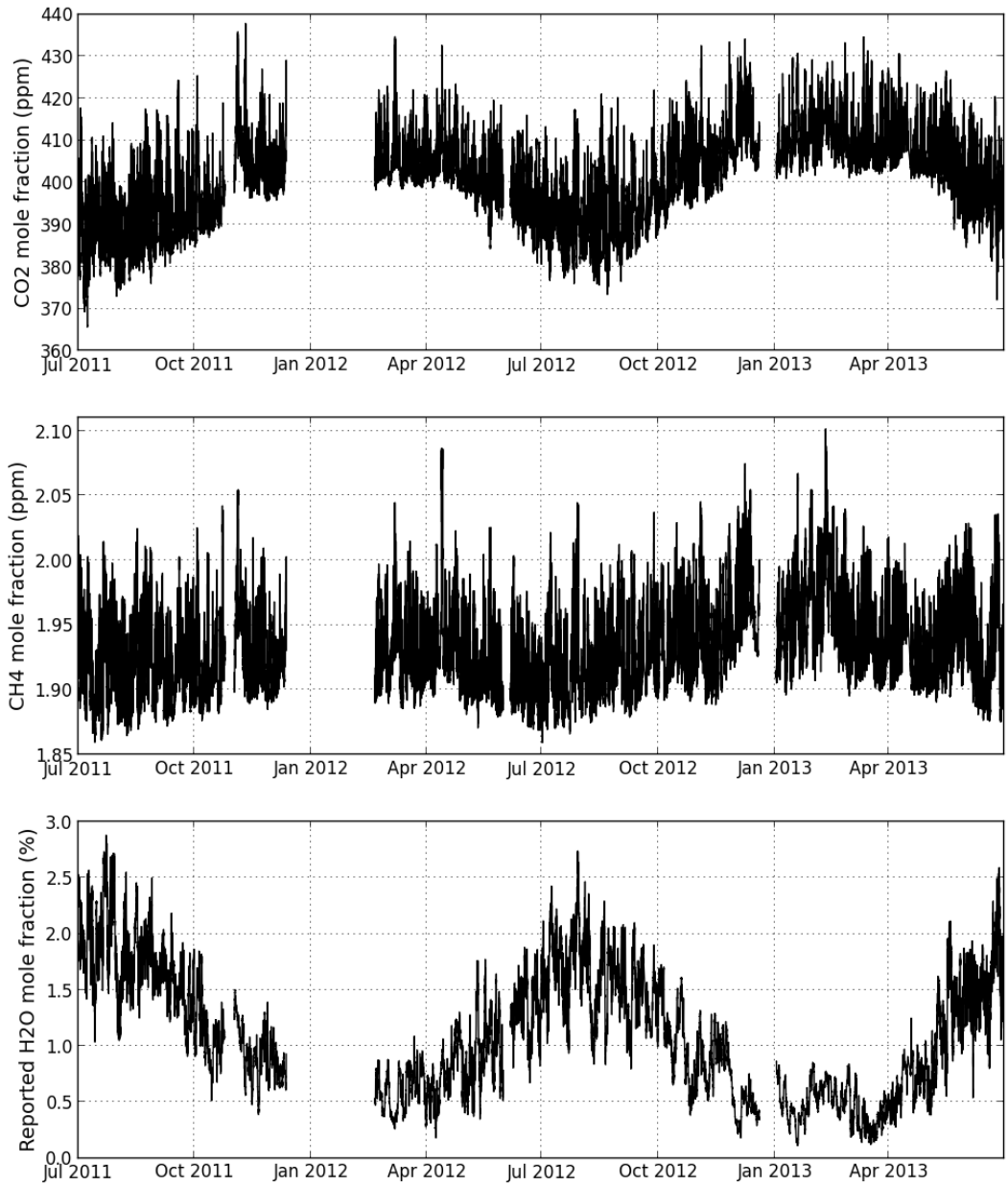

Figure 4.5. 1-min average time series of CO_2, CH_4 and reported water vapor mole fraction *measured by CFADS100 at the roof of FMI headquarters in an urban area.*

Transferability can be tested also from a different point of view, for example, by using time series data. Figure 4.5 shows the CO_2, CH_4 and water vapor time series (1-min

data). The bottom panel in Figure 4.5 is the instrument reported (not calibrated) water vapor mole fraction. If the water vapor mole fractions were corrected (Table 4.2), the actual mole fractions would be from 0.04 % (lowest mole fractions) up to 0.4 % (highest mole fractions) lower than the reported ones.

To inspect the transferability of the correction functions, the data corrected with instrument specific correction coefficients is subtracted from the data corrected with factory coefficients (Figure 4.6). The difference between the coefficients in both CO_2 and CH_4 mole fractions increases as the function of water vapor mole fraction, in addition, the plots broaden more on higher water vapor mole fractions. The difference between CO_2 mole fractions (Figure 4.6) reaches the 0.05 ppm limit at around 0.7 % water vapor mole fraction. The result is similar to the plot in middle panel in Figure 4.4 for CFADS100. For CH_4 the 1 ppb limit is reached at 1.8 % mole fraction (Figure 4.6) which is lower than in Figure 4.4 (2 %).

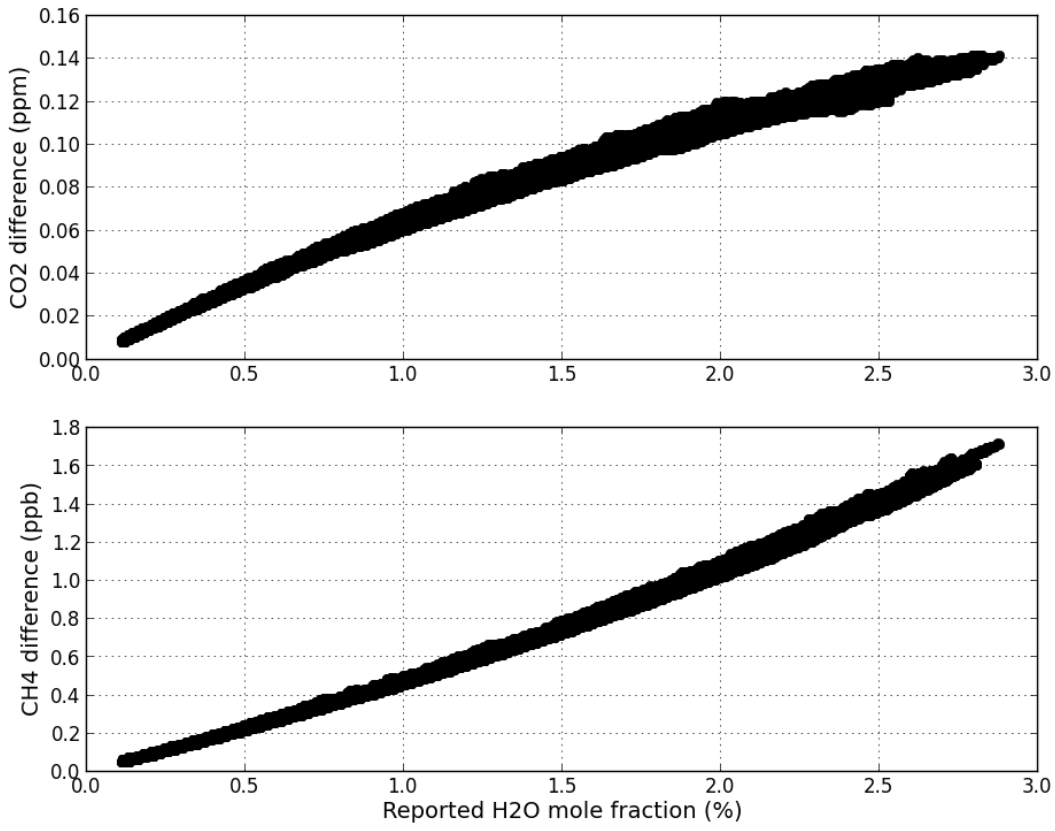

Figure 4.6. Difference in CO_2 and CH_4 dry mole fractions between water vapor correction functions determined for CFADS100 and the factory functions while using the time series data in Figure *4.5.*

Variations in atmospheric CO_2 and CH_4 mole fractions at different water vapor mole fractions cause the broadening of the plots in Figure 4.6. This can be illustrated by manipulating Equation 12:

$$C_{dry} = \frac{C_{wet}}{1 + z_1 H_{rep} + z_2 H_{rep}^2} \tag{17}$$

For example, if the factory coefficients are used and the amount of water vapor does not change (H_{rep} stays constant), but C_{wet} is changing; then C_{dry} also changes. As a result, there will be different values of mole fraction of the species on the same water vapor mole fraction. If the coefficients are changed to instrument specific ones, the resulting C_{dry} values are different than the ones acquired with factory coefficients. When the differences are calculated, there will be different values on the same water vapor mole fractions which can be seen as a broadening of the plot. In addition, the broadening increases as a function of H_{rep} (Figure 4.6). This is happening because higher H_{rep}weights the difference between the coefficients (Equation 17) more than lower H_{rep}. This phenomenon is clearer with CO_2 than with CH_4, because the dilution effect and the atmospheric variation of CH_4 are smaller. For example, at 1.0 % water vapor mole fraction the broadening of the CO_2 line is about 0.01 ppm and for CH_4 it is less than 0.1 ppb. However, at 2.0 % CO_2 broadening is almost 0.02 ppm and CH_4 broadening is 0.1 ppb. While inspecting transferability, C_{dry} was chosen to be 400 ppm. But when CO_2 mole fraction varies between 380–430 ppm, the error from this phenomenon between the equations could be ±0.01 ppm which is 10% of the WMO compatibility limits in northern hemisphere. For CH_4, the error is less than two percent.

4.4 Problems in measurements

Different kind of problems were encountered which either completely failed the measurement or did not seem to affect the results at all. All the problems happened with water droplet tests, whereas water vapor calibration measurements carried out without problems. The origin of these problems could not be verified, so the following discussion is mostly speculation.

First and the most serious problem can be described as S-motion in measurement points. In Figure 4.7, this behavior is observed between water vapor ranges 1.0–1.5 % and somewhat at 1.5–2.0 % with CO_2 but not with CH_4. This phenomenon was usually accompanied with slow water vapor mole fraction change rate during this S-motion and fast change rates on other water vapor ranges, especially on low water vapor mole fractions. Together these phenomena caused unusable coefficients and low R^2 values, therefore, measurements where this kind of behavior was encountered were ignored. During drying phase, the water vapor mole fraction usually stuck at being larger than 0.005 % and much longer drying period was required to dry the system completely. The water vapor mole fraction of the measurement in Figure 4.7 reached over 3.0 % which, according to Equation 13, corresponds to 24–25 °C dew point temperature. This is about the same as the room temperature, therefore, it is possible that water vapor condensed to pipelines, causing this behavior. When this phenomenon was first observed, the same behavior was usually observed during the next measurement and it was fixed by making the drying periods longer after measurements.

Another problem encountered in measurements was too fast evaporation of droplets at low water vapor mole fractions. For example, in Figure 4.7 it took only six minutes for water vapor mole fraction to descend from 1 % to 0.1 %. Usually this took ~20 minutes, but it has also taken over an hour in some experiments. Normally, the fast evaporation started when water vapor mole fraction was below 0.5 %. Occasionally, fast evaporation changed the state of a system too fast and, as a result, the measurement points did not go well with the fit, which caused errors in correction coefficients. These points had to be removed, but doing so limited the water vapor range of the data points, thus limiting the water vapor range the correction function describes. No extrapolation should be made as there is no way to know that the function behavior continues the same way. On few occasions, even though the fast evaporation happened at mole fractions higher than 0.5 %, the measurement points were nicely described by the fit. The reason why this fast evaporation happens at different mole fractions might be due to the placement of the droplets in the Tee-connector.

Fast evaporation did not only occur at the end of the measurements but could also occur in the middle of them. Again, this phenomenon can be seen as a gap in measurement points when plotting them, for example, in Figure 4.7 this kind of behavior was observed ~1.5 % water vapor mole fraction. This phenomenon was quite common and it did not usually cause any troubles. The size of the gaps varied and even the gaps of 0.5 % water vapor mole fractions were observed. The reason why this happened could have been due to the droplet placement during the injection. If the droplets were not injected exactly into same position inside the Tee-connector, they would cause different effective droplet area and sudden jumps in total water vapor mole fraction.

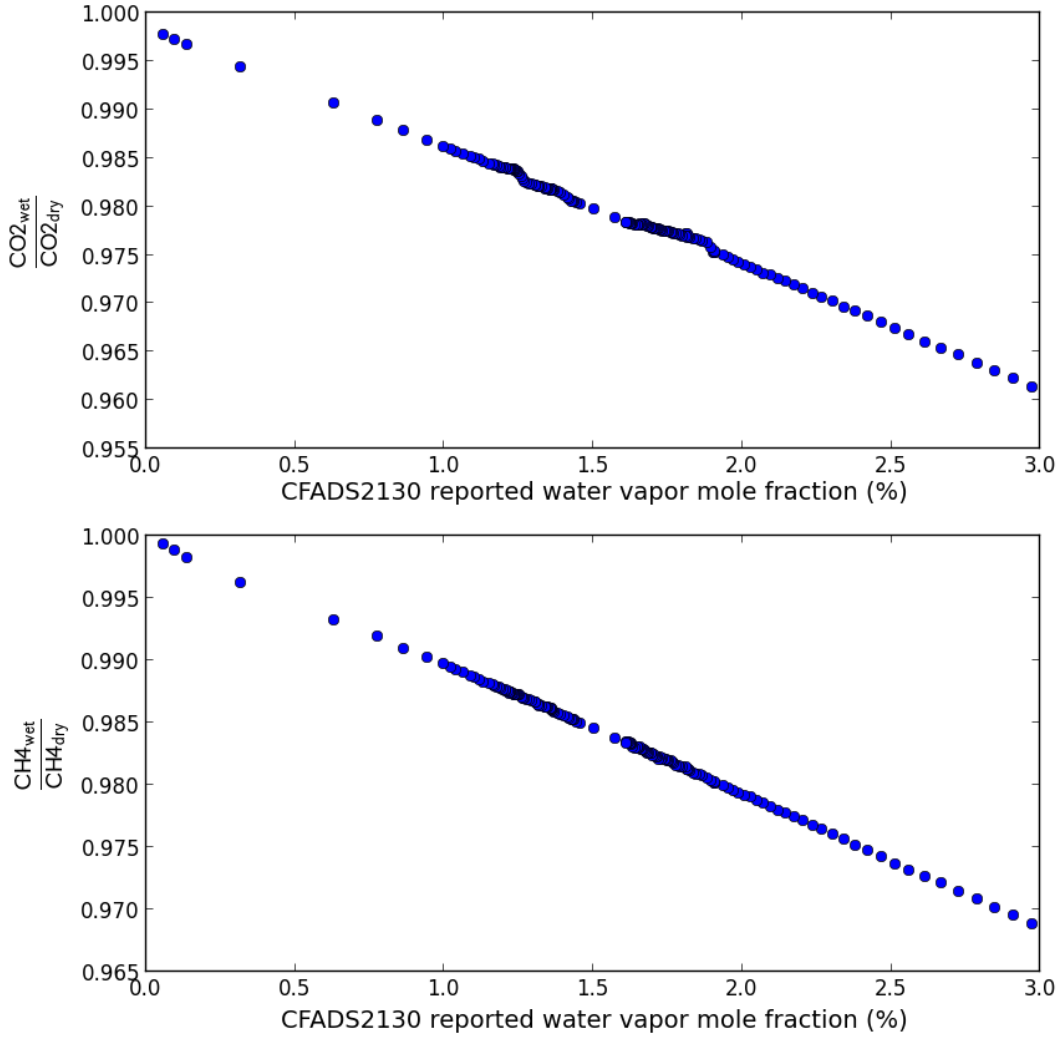

Figure 4.7. An Example plot of a failed measurement. Quadratic fit of $\frac{CO_{2wet}}{CO_{2dry}}$ *and* $\frac{CH_{4wet}}{CH_{4dry}}$ *versus reported water vapor* mole fractions *for CFADS2130. This measurement was completely ignored for both* CO_2 *and* CH_4 *and it's not included in Table C.1.*

Also, a problem in the experiment happened due to the heating of the Tee. The Tee-connector was heated after the droplet injection to raise the water vapor mole fraction to desired value (2.5 %). However, aiming to this value was sometimes difficult. After injecting the droplets, the water vapor mole fraction reported by the gas analyzer was usually ~1.4 %, but sometimes it was not same between injections, even though the injected amount of liquid water remained the same. Sometimes the water vapor mole fraction after the injection was only 1.0 % and sometimes it jumped up to 2.0 %. These numbers cannot be explained just by the variations in temperatures in the room and the Tee-system. With trial and error, it was found that stopping the heating when the reported water vapor mole fraction was ~2.0 % would make it reach 2.5 %. On the other hand, if the initial water vapor mole fraction was higher than the average one, the system required less heating which usually ended with lower water vapor mole fraction if stopped at ~2.0 %. In contrast, if the initial value was less than average, the required heating was higher than normal and if the heating was stopped at 2.0 % the final water vapor mole fraction usually ended much higher than wanted, even over 3.0 %. This happened because the change in temperature was slow in the beginning, but it increased more rapidly with time which caused rapid increase in water vapor mole fraction. In worst case scenario, this possibly caused condensation of water vapor in the pipes, thus making the measurement fail. In addition, the heating could have caused some disturbance during the time when the droplets were evaporating, because the Tee-system is also cooling down at the same time.

5 Conclusions

This study focused on investigating if the factory coefficients in Picarro analyzers are good enough to correct the dilution and line broadening effects, or if it is required to determine the correction coefficients for each analyzer separately. If the factory coefficients could be proven to be enough, it would save time and effort by not requiring doing additional measurements. Several measurements were made for seven different analyzers and the means of determined coefficients were calculated for each analyzer. These mean coefficients were compared against the factory coefficients to check, up to which water vapor mole fraction the accuracy fulfill WMO limits (WMO, 2011). In addition, water vapor calibration was carried out for all the analyzers. However, it should be noted that the water vapor calibration is not required for correcting dilution and line broadening effects and it is required only if one is interested in actual water vapor mole fraction.

The method used to carry out the water droplet test was probably not the most ideal or error-free, but it is easy to deploy and can be made on the field. One of the problems with the method is the heating of the Tee-connector, which changes the state of the system. During the drying phase, the temperature of the Tee-connector is also decreasing which affects the measured water vapor mole fraction and might cause some error in the measurement. Preferably, the droplet test should be carried out without heating and there exists many different ways to make the water droplet test in such way (e.g. Chen et al., 2010; Nara et al., 2012; Rella et al., 2012). Also, if someone requires wider water vapor range than the one used in this study (0–2.6 %), then some other method must be used. This method can reach higher dew points than the room temperature by changing the line pressure, but only up to a certain limit. To prevent the condensation on higher dew points, the room temperature should be increased and water should be injected as close to the gas analyzer as possible to minimize the length of a pipeline after the position of the liquid droplet. Also, the water vapor correction method should be standardized to minimize the differences caused by different test setups.

The results from water vapor calibration were compared to the coefficients determined

by Rella (2010) and they were quite similar. However, the first order coefficient of CFADS2135 was much larger than of the other. Before making the water vapor calibration for the gas analyzers, the dew point generator was calibrated against a chilled-mirror hygrometer. The calibration showed that the generator could not generate low and high temperatures accurately, so the calibration was applied for the generator during data analysis.

Applicability of Picarro factory water vapor correction coefficients was inspected in two different ways. In the first method, the difference between the factory correction functions and the instrument specific functions were calculated. If the difference between the functions were less than ±0.05 ppm for CO_2 and ±1 ppb for CH_4, which are half of the WMO (2011) compatibility limits, then using the factory coefficients was enough for reaching WMO limits. Because the correction function is a function of water vapor mole fraction reported by the instrument, the difference between the correction coefficients becomes more apparent when water vapor mole fraction is larger. As a result, the CO_2 factory coefficients were only good up to water vapor mole fraction of 0.7 % and for CH_4, up to 2.0 % corresponding to dew point temperature of 18 °C. Even the CH_4 factory coefficients are not good enough to use except maybe on some Arctic/Antarctic stations. Also, the CH_4 coefficients of CFADS2135 differed from others, which were assumed to be due to the difference in water vapor calibration. The second method used was a case study made with one of the analyzers and the transferability was inspected by using time series data of two years measured by the analyzer. This method gave similar results with the first one. In conclusion, it is recommended to make a water vapor correction for each instrument separately instead of using the factory correction, if the sample air is not dried. These results support the outcome of Nara et al. (2012) and Rella et al. (2012) that is the transferability was not proven or it is possible only on low humidity levels. Also, the water vapor correction should remain stable over time (Rella, 2010), so there should be no need to do the correction periodically if it is made correctly once. However, this is not verified, and currently periodic correction is recommended.

References

Adams, N.: Advances in forecasting systems at the Antarctic Meteorological Centre, Casey, *Meteorological Application*, vol. 9, Issue 3, 335-343, 2002

Berden, G., Engeln, R.: Cavity ring-down spectroscopy – techniques and applications, Blackwell *publishing Ltd*, 12, 2009

Bernath, P.: Spectra of atoms and molecules, *Oxford University Press*, New York, 1995

Bromwich, D., Nicolas, J., Monaghan, A., Lazzara, M., Keller, L., Weidner, G., Wilson, A.: Central West Antarctica among the most rapidly warming regions on Earth. *Nature Geoscience*, 6, 139-145, 2012

Busch, K. W., Busch, M. A.: Cavity Ringdown Spectroscopy: An Ultratrace Absorption Measurement Technique, *ACS Symposium Series 720*, Oxford, 1997

Chen, H., Winderlich, J., Gerbig, C., Hoefer, A., Rella, C. W., Crosson, E. R., Van Pelt, A. D., Steinbach, J., Kolle, O., Beck, V., Daube, B. C., Gottlieb, E. W., Chow, V. Y., Santoni, G. W., Wofsy, S. C.: High-accuracy continuous airborne measurements of greenhouse gases (CO_2 and CH_4) using the cavity ring-down spectroscopy (CRDS) technique, *Atmospheric Measurement Techniques*, Volume 3, Number 2, 375-386, 2010

Crosson, E. R.: A cavity ring-down analyzer for measuring atmospheric levels of methane, carbon dioxide and water vapor, *Appl. Phys.*, B 92, 403-408, 2008

Crutzen, P.J.: Methane's sinks and sources, *Nature*, 350, 380-381, 1991

Dicke, R.: The effect of collisions upon the Doppler width of spectral lines, *Phys. Rev.*, 89, 472–473, 1953

Forster, P., Ramaswamy, V., Artaxo, P., Berntsen, T., Betts, R., Fahey, D.W., Haywood, J., Lean, J., Lowe, D.C., Myhre, G., Nganga, J., Prinn, R., Raga, G., Schulz M., Van Dorland, R.: Changes in Atmospheric Constituents and in Radiative Forcing. In: Climate Change 2007: The Physical Science Basis. Contribution of Working Group I to the Fourth Assessment Report of the Intergovernmental Panel on Climate Change [Solomon, S., Qin, D., Manning, M., Chen, Z., Marquis, M., Averyt, K.B., Tignor, M., Miller H.L. (eds.)]. Cambridge University Press, Cambridge, United Kingdom and New York, NY, USA, 137-143, 2007

Frankenberg, C., Bergamaschi, P., Butz, A., Houweling, S., Meirink, J. F., Notholt, J., Petersen, A. K., Schrijver, H., Warneke, T., and Aben, I.: Tropical methane emissions: A revised view from SCIAMACHY onboard ENVISAT, *Geophys. Res. Lett.*, 35, 2008

Galatry, L.: Simultaneous effect of Doppler and foreign gas broadening on spectral lines, *Phy. Rev*. 122, 1218–1223, 1961

Houweling, S., Rockmann, T., Aben, I., Keppler, F., Krol, M., Meirink, J. F., Dlugokencky, E. J., and Frankenberg, C.: Atmospheric constraints on global emissions of methane from plants, *Geophys. Res. Lett.*, 33, 2006

Goff, J. A., and Gratch S.: Low-pressure properties of water from −160 to 212 °F, *Transactions of the American Society of Heating and Ventilating Engineers*, 95–122, New York, 1946

Goff, J. A.: Saturation pressure of water on the new Kelvin temperature scale, *Transactions of the American Society of Heating and Ventilating Engineers*, 347–354, 1957

Heinonen, M.: Uncertainty in humidity measurements, *Publication of the EUROMET workshop P758*, MIKES J4/2006, Centre for metrology and accreditation, 2006

Huntingford, C., Lowe, J. A., Booth, B. B. B., Jones, C. D., Harris, G. R., Gohar, L. K., and Meir, P.: Contributions of carbon cycle uncertainty to future climate projection spread, *Tellus*, 61B(2), 355–360, 2009

Kiehl, J. T. and Trenberth, K. E.: Earth's annual global mean energy budget, *Bulletin of the American Meteorological Society*, 78(2), 197–208, 1997

Klausen, J., Scheel, H.E., Steinbacher, M.: WMO/GAW glossary of QA/QC-related terminology, 2010, retrieved 7.10.2013 from http://gaw.empa.ch/glossary/glossary.html

Montzka, S. A., Dolugokencky, E. J., Butler J. H.: Non-CO2 greenhouse gases and climate change, *Nature*, 476, 43-50, 2011

Nara, H., Tanimoto, H., Tohjima, Y., Mukai, H., Nojiri, Y., Katsumata, K., Rella, C. W.: Effect of air composition (N2, O2, Ar, and H2O) on CO2 and CH4 measurement by wavelength-scanned cavity ring-down spectroscopy: calibration and measurement strategy, *Atmospheric Measurement Techniques*, vol. 5, Issue 11, 2689, 2012

O'Keefe, A., Deacon, D. A. G.: Cavity ring-down optical spectrometer for absorption-measurements using pulsed laser sources. *Review of Scientific Instruments*, 59, 2544–2551, 1988

Picarro Inc.: Cavity Ring-Down Spectroscopy CRDS, retrieved 7.10.2013, from http://www.picarro.com/technology/cavity_ring_down_spectroscopy

Picarro Inc.: WS-CRDS – A Universal Instrument for Precision Measurement of GHGs, 2010, retrieved 7.10.2013 from http://www.picarro.com/sites/default/files/GHG_whitepaper.pdf

Rautian S. G., Sobel'man I. I.: "The effect of collisions on the doppler broadening of spectral lines" *Sov. Phys. Usp.* **9,** 701–716, 1967

Rella C. W.: Accurate greenhouse gas measurements in humid gas streams using the picarro G1301 carbon dioxide / methane / water vapor gas analyzer, Picarro Inc., 2010, retrieved 7.10.2013 from http://www.picarro.com/assets/docs/White_Paper_G1301_Water_Vapor_Correction.pdf

Rella, C. W., Chen, H., Andrews, A. E., Filges, A., Gerbig, C.,Hatakka, J., Karion, A., Miles, N. L., Richardson, S. J., Steinbacher, M., Sweeney, C., Wastine, B., Zellweger, C.: High accuracy measurements of dry mole fractions of carbon dioxide and methane in humid air, *Atmospheric Measurement Techniques*, Vol. 5 Issue 4, 5823, 2012

Richardson, S. J., Miles, N. L., Davis, K. J., Crosson, E. R., Rella, C. W., Andrews, A. E.: Field testing of cavity ring-down spectroscopy analyzers measuring carbon dioxide and water vapor, *J. Atmos. Ocean. Tech*, 397-406, 2011

Scherer, J., Paul, J., O'Keefe, A., Saykally, R.: Cavity ring-down laser absorption spectroscopy: history, development, and application to pulsed molecular beams, *Chem. Rev.*, 97, 25-51, 1997

Schwartz S. E., Warneck P.: Units for use in atmospheric chemistry (IUPAC Recommendations 1995). International Journal of Pure and Applied Chemistry 67 (8/9), 1377-1406, 1995

Silver, J. A.: Frequency-modulation spectroscopy for trace species detection – theory and comparison among experimental methods. *Applied Optics*, 31, 707– 717, 1992

Stephens, B. B., Miles, N. L., Richardson, S. J., Watt, A. S., and Davis, K. J.: Atmospheric CO2 monitoring with single-cell NDIR-based analyzers. *Atmos. Meas. Tech. Discuss.*, 4, 4325–4355, 2011

Tans, P. P., Bakwin, P. S., Guenther, D. W.: A feasible global carbon cycle observing system: A plan to decipher today's carbon cycle based on observations, *Glob. Change Biol.*, 2, 309–318, 1996

Varghese, P. L., Hanson, R. K.: Collisional narrowing effects on spectral line shapes measured at high resolution, *Appl. Optics*, 23, 2376, 1984

Vaughn, B. H., Crosson, E. R., White, J. W., Sweeney, C.: Wavelength-Scanned Cavity Ring Down Spectroscopy: Opening new doors for tracing water isotopes in

the hydrosphere, biosphere and atmosphere, *American Geophysical Union*, Fall Meeting, 2008

VIM: International vocabulary of metrology – Basic and general concepts and associated terms, 3rd Edition, 2012

Vinther, B. M., Andersen, K. K., Jones, P. D., Briffa, K. R., Cappelen J.: Extending Greenland temperature records into the late eighteenth century, *J. Geophys. Res.*, 111, D11105, 2006

Wheeler, M. , Newman, S., Orr-Ewing, A., Ashfold, M.: Cavity ring-down spectroscopy, *J. Chem. Soc.*, Faraday Trans. 94, 337-351, 1998

Winderlich, J., Chen, H., Gerbig, C., Seifert, T., Kolle, O., Lavric, J. V., Kaiser, C., Höfer, A.,and Heimann, M.: Continuous low-maintenance CO2/CH4/H2O measurements at the Zotino Tall Tower Observatory (ZOTTO) in Central Siberia, *Atmos. Meas. Tech.*, 3, 1113–1128, 2010

WMO: Report of the 15th WMO/IAEA Meeting of Experts on Carbon Dioxide, Other Greenhouse Gases, and Related Tracers Measurement Techniques, 7–10 September 2009, GAW Report No. 194, WMO TD No. 1553, Jena, Germany, 2011

WMO: Technical Regulations, Basic Documents No. 2, Volume I – General Meteorological Standards and Recommended Practices, 2011 edition, Updated in 2012, 31, retrieved 7.10.2013 from http://library.wmo.int/pmb_ged/wmo_49-v1-2012_en.pdf

Zalicki P., Zare R.: Cavity ring-down spectroscopy for quantitative absorption measurements, *J. Chem. Phys.*, 102, 2708, 1995

Appendix A : Terminology

Standardization is important when evaluating and characterizing data to ensure the comparability and compatibility of measurements. If terms are used with a different meaning, it could make the reader to misinterpret what was written. Some of the relevant terms concerning this study are explained according to Klausen et al. (2010) and VIM (2012). These definitions have also been recommended for use by the GAW program of the WMO.

Accuracy: Closeness of agreement between a measured quantity value and a true quantity value. A measurement is more accurate when it has a smaller measurement error.

Bias: Estimate of a systematic measurement error.

Comparability: Measurement results are comparable when results of different measurements are traceable to the same measurement unit, for example, the metre.

Compatibility: Property of a set of measurement results for a specified measured quantity, such that the absolute value of the difference of any pair of measured quantity values from two different measurement results is smaller than some chosen multiple of the standard measurement uncertainty of that difference.

Concentration: Amount of substance per unit volume of air. Concentration can be, for example, mass $\left(\frac{kg}{m^3}\right)$, number $\left(\frac{1}{m^3}\right)$ or mole $\left(\frac{mol}{m^3}\right)$ concentration. So, it is wrong to say: "The concentration of CO_2 in the air is 400 ppm. This refers to the dry air mole fraction of CO_2 and it is not a concentration.

Mixing ratio: Can be either mass or volume mixing ratio, so further specification is needed when using it. Mass mixing ratio describes the number of the mass of the target gas per mass of air. Volume mixing ratio describes number of molecules of the target gas per fixed number of air molecules in unit volume. Also, a

specification whether the air is dry or moist is required. Possible units are ppm, ppb, %, etc.

Mole fraction: Relative number of molecules of certain chemical in a fixed number of air molecules. Volume has nothing to do with mole fraction. Also, a specification whether the air is dry or moist is required. Possible units are ppm, ppb, $\frac{mol}{mol}$, %, etc. Mole fractions are habitually referred to as mixing ratios, but it should be avoided as term mole fraction does not require an assumption of ideality of gases and it is also applicable to condensed-phase species (Schwartz and Warneck 1995).

Precision: Closeness of agreement between measured quantity values obtained by replicate measurements on the same objects under specified conditions.

Sensitivity: Quotient of the change in an indication of a measuring system and the corresponding change in a value of a measured quantity. It can depend on the value of the quantity being measured.

Systematic measurement error: A measurement error which varies with a predictable manner in replicate measurements.

Uncertainty: Non-negative parameter describing dispersion of the quantity values being attributed to a measured value. The parameter can be, for example, a standard deviation called standard measurement uncertainty.

Appendix B: The difference between dilution and line broadening effects

If the water vapor calibration and the water droplet test have been made, it is possible to calculate the error caused by dilution (Chapter 2.2.1) and line broadening effects (Chapter 2.2.2) separately. From Equation 9, one can calculate a diluted mole fraction ($C_{diluted}$) by measuring a dry mole fraction C_{dry} and doing water vapor calibration from where values of H_{act} can be acquired. An error caused by the dilution effect can be calculated with following equation:

$$E_{dilution} = C_{dry} - (1 - 0.01 * H_{act}) * C_{dry} \quad (18)$$

where the term inside the brackets is also known as a diluted mole fraction ($C_{diluted}$). Also, the error caused by line broadening effects can be calculated by assuming that the rest of the error between wet and dry mole fractions is caused by those effects. So, the error caused by line broadening effects is:

$$E_{spec} = (1 - 0.01 * H_{act}) - C_{wet} \quad (19)$$

where C_{wet} can be acquired from the droplet test.

These errors were calculated for the same dataset of CFADS2242, which was used to illustrate the results in the results section. For both CO_2 and CH_4, the calculated dilution effect is larger than the line broadening effects (Figure 4.3), which was expected. However, when the water vapor mole fraction is low (< 0.02 %) the line broadening effects are larger than the dilution effect. On the other hand, the ratio of error caused by dilution and line broadening effects differ between CO_2 and CH_4. For CO_2, the dilution effect is twice as large as line broadening effects and the ratio stays about the same for the whole water vapor range. In contrast, the ratio of these effects is not constant for CH_4. At 0.5 % water vapor mole fraction, the dilution effect is three times larger than the line

broadening effects, but at 2.5 %, the dilution effect is almost five times larger.

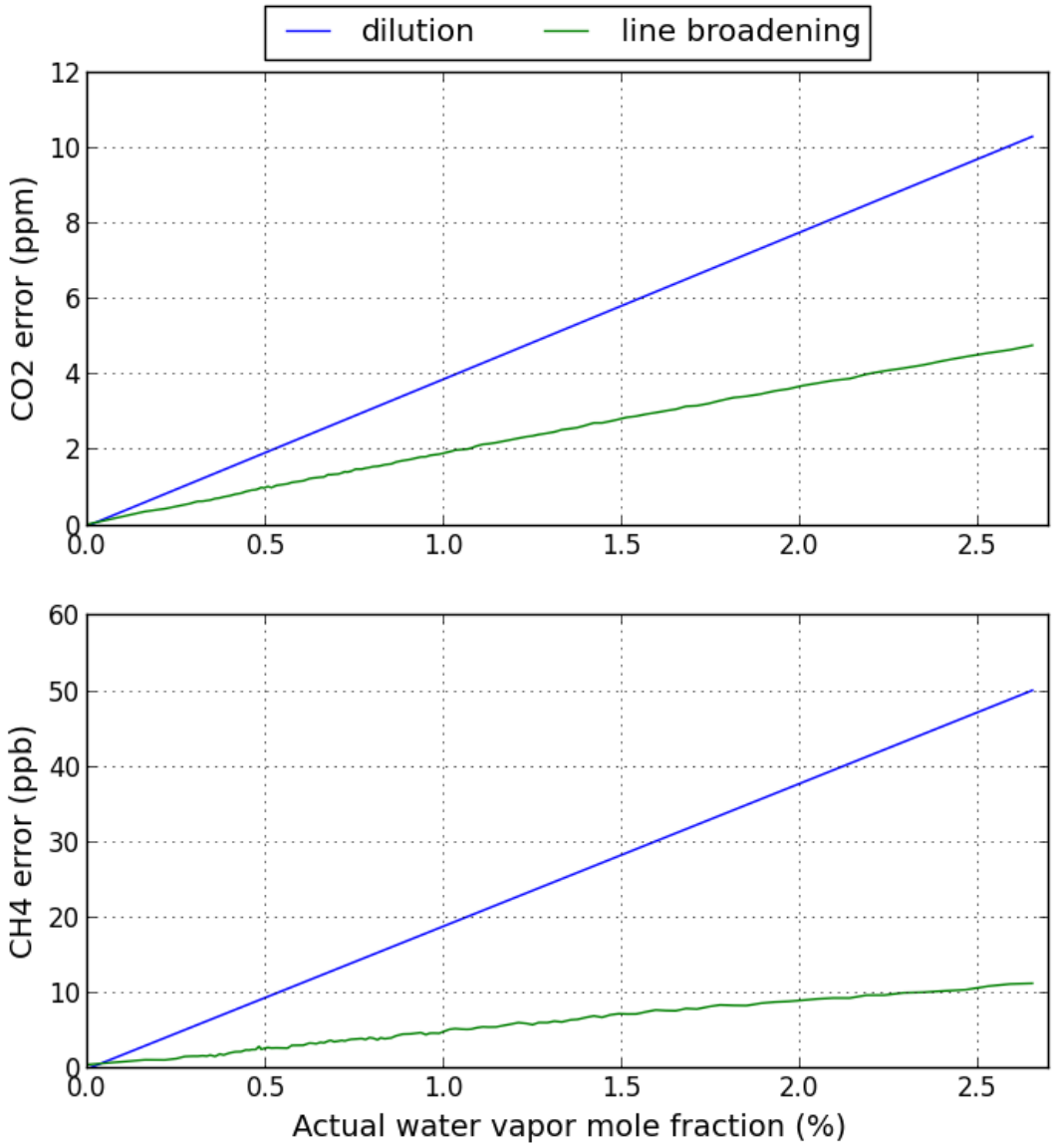

Figure B.1. Amount of error caused by dilution (blue) and line broadening effects (green) for CO_2 and CH_4 on different water vapor mole fractions acquired from example data of CFADS2242. In this case, the water vapor mole fraction is the actual mole fraction and not the one reported by the analyzer.

Appendix C: List of water vapor correction coefficients

Table C.1. All the water vapor correction coefficients acquired from water droplet tests made for the gas analyzers. First number in CO_2 and CH_4 columns is the second order coefficient and the second number is the first order coefficient. Cells colored red were excluded when calculating the mean values and standard deviation of the coefficients because the fit had $R^2 < 0.999$. The table does not include the coefficients from the fits which had R^2 value less than 0.999 for both CO_2 and CH_4.

Instrument	Date	CO_2		CH_4	
		z_2	z_1	z_2	z_1
CFADS100					
	20.9.2012	-0.0002474	-0.01189	-0.0002650	-0.00946
	30.11.2012	-0.0003149	-0.01177	-0.0001991	-0.00964
	18.1.2013	-0.0003002	-0.01181	-0.0001877	-0.00969
	18.1.2013	-0.0003655	-0.01151	-0.0001961	-0.00963
	Mean	-0.0002875 ± 0.0000205	-0.01182 ± 0.00004	-0.0002120 ± 0.0000179	-0.00961 ± 0.00005
CFDDS101					
	11.10.2012	-0.0002948	-0.01180	-0.0001476	-0.00974
	17.10.2012	-0.0002846	-0.01185	-0.0001239	-0.00976
	9.11.2012	-0.0003185	-0.01171	-0.0002763	-0.00935
	Mean	-0.0002993 ± 0.0000100	-0.01179 ± 0.00004	-0.0001358 ± 0.0000118	-0.00975 ± 0.00001
CFADS2130					
	12.10.2012	-0.0002010	-0.01208	-0.0000685	-0.01039
	19.10.2012	-0.0002406	-0.01200	-0.0000469	-0.01050
	8.11.2012	-0.0002246	-0.01204	-0.0000421	-0.01048
	14.12.2012	-0.0002316	-0.01200	-0.0000005	-0.01055
	Mean	-0.0002244 ± 0.0000085	-0.01203 ± 0.00002	-0.0000395 ± 0.0000142	-0.01048 ± 0.00004
CFADS2135					
	17.10.2012	-0.0001908	-0.01217	0.0000268	-0.01072
	21.11.2012	-0.0001954	-0.01216	0.0000516	-0.01073
	22.11.2012	-0.0001985	-0.01214	0.0001858	-0.01111
	29.11.2012	-0.0001925	-0.01217	0.0000868	-0.01086
	17.12.2012	-0.0002324	-0.01208	0.0000490	-0.01081
	18.12.2012	-0.0002250	-0.01207	0.0000646	-0.01082
	Mean	-0.0002057± 0.0000074	-0.01213 ± 0.00002	0.0000558 ± 0.0000249	-0.01079 ± 0.00003
CFADS2237					
	14.9.2012	-0.0002434	-0.01202	-0.0001036	-0.01038
	18.10.2012	-0.0002223	-0.01217	-0.0001359	-0.01031
	15.11.2012	-0.0001735	-0.01220	-0.0000349	-0.01086
	Mean	-0.0002131 ± 0.0000207	-0.01213 ± 0.00006	-0.0001197 ± 0.0000161	-0.01034 ± 0.00004
CFADS2242					
	13.9.2012	-0.0002474	-0.01209	-0.0001011	-0.01042
	14.9.2012	-0.0002206	-0.01214	-0.0001902	-0.01013
	11.10.2012	-0.0003686	-0.01190	-0.0001377	-0.01024
	Mean	-0.0002789 ± 0.0000455	-0.01204 ± 0.00007	-0.0001430 ± 0.0000448	-0.01026 ± 0.00015
CFKADS2066					
	3.10.2012	-0.0001908	-0.01213	-0.0001452	-0.00972
	4.10.2012	-0.0002249	-0.01204	-0.0001687	-0.00961
	4.10.2012	-0.0002522	-0.01200	-0.0002017	-0.00959
	Mean	-0.0002227 ± 0.0000178	-0.01206 ± 0.00003	-0.0001719 ± 0.0000164	-0.00964 ± 0.00004